Charles University in Prague
Faculty of Science

DIPLOMA THESIS

Petra Bačová

Linear semiflexible polyelectrolytes in solutions
Lineární semiflexibilní polyelektrolyty v roztocích

Department of Physical and Macromolecular Chemistry

Supervisor: Doc. Ing. Zuzana Limpouchová, CSc.
Consultant: Mgr. Peter Košovan, PhD.

Branch of study: Physical chemistry

2010

I would like to show my gratitude to my supervisor, Zuzana Limpouchová, for her support and helpful advices from the initial to the final level of my work. I am also grateful to my consultant, Peter Košovan, this thesis would not have been possible without him. Great thanks to my professor, Karel Procházka, for his help, patience and time, that he spent with the never-ending corrections of the thesis. It was a pleasure for me to work in our lab with all the admirable people. This work was supported by the Grant Agency of the Czech republic, grant 43-257269, thanks to all.

I declare that I have written my diploma thesis by myself and that all the sources of information used are listed in the bibliography. I agree that this work may be lent and published.

In Prague Petra Bačová

Contents

Title: Linear semiflexible polyelectrolytes in solutions
Author: Petra Bačová
Department: Faculty of Science, Charles University in Prague
Supervisor: Doc. Ing. Zuzana Limpouchová, CSc.
Supervisor's e-mail address: zl@vivien.natur.cuni.cz
Consultant: Mgr. Peter Košovan, PhD.

Abstract:

In the thesis, molecular dynamics simulations are used for studying the charged linear polymers (polyelectrolytes) and their conformational behavior in solutions. The study focuses on semiflexible chains, because they have not been studied as systematically as the flexible or stiff polyelectrolytes. The persistence length is a characteristic of chain flexibility which is influenced by intrinsic chain stiffness and by electrostatic interactions of charged monomer units. In the thesis, the conformational behaviour of polyelectrolytes in solutions differing in the salt concentration is simulated and the effect of ionic strength on the conformational behaviour is studied. The persistence length of semiflexible polymer is calculated using several different definitions and the results are compared. Salt ions are treated implicitly within the Debye-Hückel approximation. The simulation results are compared with the Odijk-Skolnick-Fixman theory and with the conclusions of the variational approach of Manghi and Netz. The results confirm the theoretically predicted double exponential decay of the orientation correlation function. The roles of the intrinsic and electrostatic persistence lengths are analyzed and their effects on the conformational behavior are discussed in detail.

Keywords: polyelectrolytes, persistence length, simulations, salty solutions

Název: Lineární semiflexibilní polyelektrolyty v roztocích
Řešitel: Petra Bačová
Ústav: Katedra fyzikální a makromolekulární chemie
Školitel: Doc. Ing. Zuzana Limpouchová, CSc.
E-mail školitele: zl@vivien.natur.cuni.cz
Konzultant: Mgr. Peter Košovan, PhD.

Abstrakt:

V diplomové práci jsou studovány lineární nabité polymery (polyelektrolyty) a jejich konformační chování v roztocích pomocí počítačových simulací metodou molekulární dynamiky. Studie je zaměřena na semiflexibilní řetězce, které nebyly prostudovány tak systematicky jako flexibilní nebo tuhé polyelektrolyty. Perzistenční délka charakterizuje ohebnost řetězce, kterou ovlivňuje jednak vnitřní tuhost řetězce a jednak elektrostatické interakce nabitých monomerních jednotek. V práci je simulováno konformační chování v roztocích lišících se koncentrací soli a je studován vliv iontové síly na konformační chování polyelektrolytů. Pro výpočet perzistenční délky je použito několik různých definic a výsledky jsou porovnány. Elektrostatické interakce jsou popsány pomocí Debye-Hückelovy aproximace. Výsledky simulací jsou porovnány s Odijk-Skolnick-Fixmanovou teorií a se závěry variačních výpočtů Mangiho a Netze. Výsledky potvrzují dvouexponenciální průběh orientační korelační funkce plynoucí z teorie. Je analyzována role vnitřní a elektrostatické perzistenční délky a je podrobně diskutován její vliv na konformační chování.

Klíčová slova: polyelektrolyty, perzistenční délka, simulace, zasolené roztoky

List of Symbols

ΔE_{bend}	elastic bending energy per unit length of the chain
Δt	time step
ϵ	parameter describing steepness of WCA potential
Γ	friction coefficient
κ^{-1}	Debye screening length
κ_b	bending modulus of polymer
λ_1,λ_2	parameters in Dobrynin's expression of the orientational correlation function
ϕ	bond angle
ϕ_0	equilibrium value of bond angle
ρ	number density of particles
σ	diameter of beads
σ_{l_p}	standard deviation of persistence length
τ	value of argument of the autocorrelation function for which the function equals e^{-1}
R_c	radius of curvature
θ	complementary angle to the bond angle
ε_0	vacuum permittivity
ε_r	relative dielectric constant of the medium
A	universal symbol for calculated quantity
a, b	parameters of linear functions used for fits
B	parameter in Manghi's and Netz's expression of the orientational correlation function
c	number of saved configurations between two studied conformations
$C(c)$	autocorrelation function of end-to-end distance

d	number of degrees of freedom
e	unit charge
f	fraction of charged monomeric units
I	ionic strength
j	distance between two bond vectors
k	position on the chain
k_B	Boltzmann constant
k_{bend}	bending constant
k_{FENE}	parameter of bonding potential
l	bond length
l_b	Bjerrum length
l_p	universal symbol for persistence length
l'_p	apparent persistence length obtained from experiment
$l_p(k)$	local persistence length
l_p^0	intrinsic persistence length
l_p^e	electrostatic persistence length
l_p^t	total persistence length
m_i	mass of i-th particle
N	number of bond vectors
n_c	total number of saved configurations
N_m	number of monomeric units per chain
n_s	number of time steps
R_{FENE}	maximum bond stretching
r_{cut}	WCA cut-off distance
r_{ij}	distance between the i-th and j-th particle
s	distance along the chain contour
s_c	crossover length
T	temperature of the system
t	universal symbol for time

T_k	kinetic temperature
t_s	simulation time
$U(\phi)$	angle potential
$U(\mathbf{R}^N)$	interaction potential
$U_{\mathrm{DH}}(r_{ij})$	Debye-Hückel potential
U_{FENE}	attractive finitely-extensible non-linear elastic (FENE) potential
U_{WCA}	Weeks-Chandler-Andersen potential
V	volume of the system
$\mathbf{F}_i^r(t)$	stochastic force on i-th particle
$\mathbf{F}_i$	force on the i-th particle
$\mathbf{R}_e$	end-to-end vector
$\mathbf{R}_g$	radius of gyration
$\mathbf{R}_i$	position vector of i-th particle
$\mathbf{r}_i$	i-th bond vector between $(i-1)$-th and i-th particle
$\mathbf{R}_{cm}$	position vector of the center of mass
$\mathbf{v}_i$	velocity of particle i
$R_{\max}$	contour length
FJC	freely jointed chain
OCF	orientational correlation function
OSF	Odijk, Skolnick, Fixman
PEs	polyelectrolytes
WCA	Weeks-Chandler-Andersen

1. Introduction

For many years, people have been using polymers without realizing, that they have been using a special material with extraordinary properties. Biopolymers such as cellulose or natural rubber and also synthetic polymers found applications in various industrial sectors. [1] Nowadays there are many polymer products which help us in everyday life. They offer a number of benefits to almost all, women appreciated the invention of nylons, tires changed men's world and the top-quality nappies make the children's life happier. The research of new polymer materials opens new possibilities for scientists, macromolecules with desired properties are synthesized and polymer physics helps to understand the behaviour of biopolymers such as DNA or proteins.

Linear polymer is a long chain that is composed of repeating units, called monomeric units, connected by covalent bonds. Linear polymer chain in a solution can form a number of different conformations (spatial arrangements). [2] Polyelectrolytes are polymers that contain charged or ionizable groups in their chains. They are usually water-soluble and due to the long-ranged electrostatic interactions the description of their properties in solutions is more complicated than that of neutral polymers. [3] The repulsion of charges along the chain has an effect on its flexibility, because it leads to chain stretching. When a salt is added to the solution, the electrostatic interactions are screened by the ions of salt and it causes conformational changes of the chain. [4] In spite of a large scientific effort over the last years, the understanding of the behaviour of polyelectrolytes in solutions is still poor.

Molecular simulations represent an important step in the study of polyelectrolytes. [5] They allow to predict, analyze and explain the properties of polymers thanks to mathematical and statistical approaches. The results of simulations can prove the theoretical assumptions and they can be used for testing the theories. The simulations can spare a lot of time and finances, because the simulation data offer basic information about a polymer chain before it is actually synthesized or studied experimentally. For example, the stiffness of polyelectrolytes is a property that is quite difficult to quantify under various conditions and not very well described by theory, so the molecular simulations are a perfect tool for its investigation.

The chain stiffness can be characterized by the persistence length. [6] The persistence length expresses the ability of bending of the chain and tells us something about the possible conformations of polymers in solutions. There are many theories of the persistence length and different ways how to define it. [7] In case of semiflexible polyelectrolytes, two contributions to the chain stiffness have to be taken into account: intrinsic stiffness of the chain and the contribution due to the electrostatic repulsion of charged monomeric units. The most known theory of the persistence length was derived by Odijk, Skolnick and Fixman (OSF) [8, 9]. It assumes that the total persistence length is a sum of two contributions: electrostatic and intrinsic persistence length. Many studies have been based on this theory and have been focused on the dependence of the electrostatic persistence

length on the ionic strength of solution. This dependence is particularly helpful in biochemistry. For example, the stiffness of DNA or other biopolymer could be moderated by suitable choice of conditions and it could influence the biological function of DNA. [10] It is possible to obtain this dependence from experiment as well. [11, 12, 13] Recently published results show that the electrostatic persistence length is scale dependent. It is an important fact that can explain why the bond-angle correlation function calculated from simulation data of semiflexible polyelectrolytes doesn't follow the single exponential decay as was predicted by OSF. [14] As a result we can observe different behaviour of polyelectrolytes at short length scales (controlled by intrinsic stiffness) and at long length scales (electrostatic contribution). This two-scale behaviour was the topic of the study of Manghi and Netz (variational theory) [15] and Dobrynin (simulation and variational theory) [16]. At present most experimental techniques are able to measure only the stiffness of polymers at long scales, so the two-scale behaviour hasn't been confirmed by measurement yet.

2. Aims of the thesis

The thesis is aimed at information allowing better understanding of the conformational behavior of linear semiflexible polyelectrolytes in salty solutions. For this purpose, extensive molecular dynamics simulations were performed and the orientation correlation function (OCF) was calculated for different values of the ionic strength and intrinsic stiffness of polyelectrolyte chains.

The goal of a careful analysis of OCF decays is to elucidate the effect of the two aforementioned characteristics on the conformational behavior. The simulated function was used also for testing the validity of the Odijk-Skolnick-Fixman theory and of the conclusions of the variational approach of Manghi and Netz.

3. Models of polymer chains

A polymer chain consists of a large number of building units and has a high molecular weight. When we study such large system, we are usually interested in global characteristics only and we don't go in details. We choose an appropriate model that includes the information on the polymer structure (connectivity, charge of monomeric unit etc.) and interactions in the system, but is simple enough to describe the chain properties.

One of the simplest models is a model of ideal chain. [2] The ideal chain is modeled by jointed links, they interact neither with each other nor with solvent. The model can be applied in some cases also for real polymers. Real chains behave like ideal under so called theta conditions. Theta condition for polymers corresponds to the state, at which the attractive and repulsive interactions between monomeric units cancel each other. The condition can be fulfilled by a suitable choice of the solvent and temperature. [17]

Another possibility how to model a polymer chain is to applied a coarse-graining method. [18] A coarse-grained polymer model consists of units that have non-zero volume and interactions in system are described by an appropriate force field. It allows to solve the problems relating to real polymers.

This section deals with both models used in my study, the first one gives basic theoretical expressions for further calculations and the second one is implemented in simulations.

3.1 Ideal chain

Let's consider a polymer chain consisting of $N+1$ monomeric units. The position of every monomeric unit is given by position vector $\mathbf{R}_i$. Usually it is better to express the configuration of polymer as a set of bond vectors $\{\mathbf{r}_i\}$=($\mathbf{r}_1$...$\mathbf{r}_N$) with the same length denoted as l. [19] The bond vector is a vector between consequent monomeric units:

$$\mathbf{r}_i = \mathbf{R}_i - \mathbf{R}_{i-1} \quad i = 1, 2, 3..N,$$

$$|\mathbf{r}_i| = l.$$

We replace the system of connected monomeric units by a model of chain represented by N joined bond vectors without mass and volume. [19] The process is schematically depicted in Fig. 3.1.

The size of the chain can be characterized by the radius of gyration $\mathbf{R}_g$ and end-to-end distance $\mathbf{R}_e$. [2] Both of them are characteristics of ideal chains as well as real polymers. The square radius of gyration is defined as an average squared distance between monomeric units in a given conformation and the polymer's center of mass (see Fig 3.1):

$$\mathbf{R}_g^2 = \frac{1}{(N+1)} \sum_{i=0}^{N} (\mathbf{R}_i - \mathbf{R}_{cm})^2. \tag{3.1}$$

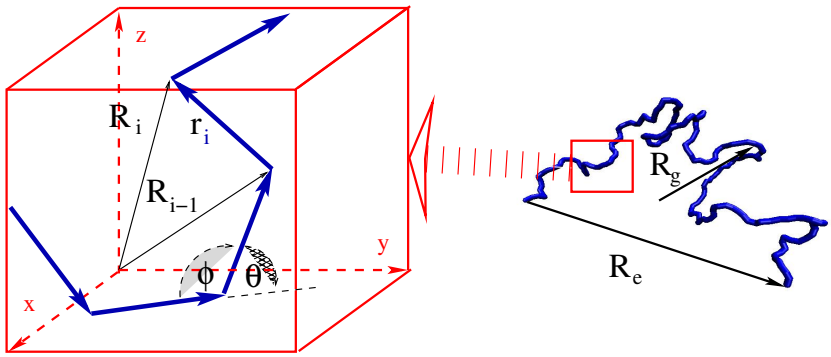

Figure 3.1: Model of ideal chain

$\mathbf{R}_i$ and $\mathbf{R}_{cm}$ are position vectors of i-th monomeric unit and center of mass. The end-to-end distance is a vector connecting the ends of a linear polymer chain in a particular conformation:

$$\mathbf{R}_e = \mathbf{R}_N - \mathbf{R}_0 = \sum_{i=1}^{N} \mathbf{r}_i. \tag{3.2}$$

The maximum value of the end-to-end distance of a fully extended linear chain is called the contour length $R_{\max}$. The probability, that a chain forms a fully stretched conformation in solution, is very low. There is a huge number of different conformations of the chain in solution and so in order to obtain relevant information on the chain size and structure, an average value of the end-to-end distance and radius of gyration is calculated. The mean-square end-to-end distance $\langle \mathbf{R}_e^2 \rangle$ is given by:

$$\langle \mathbf{R}_e^2 \rangle = \sum_{i=1}^{N} \sum_{j=1}^{N} \langle \mathbf{r}_i \cdot \mathbf{r}_j \rangle = \sum_{i=1}^{N} \langle \mathbf{r}_i^2 \rangle + 2 \sum_{i>j} \langle \mathbf{r}_i \cdot \mathbf{r}_j \rangle. \tag{3.3}$$

The equations mentioned above are valid generally for every polymer chain. Under specific conditions they can be modified and we obtain a simple expression for particular model of ideal chain:

- **Freely jointed chain**: there are no correlations between the directions of different bond vectors $\mathbf{r}_i$ and $\mathbf{r}_j$, thus $\langle \mathbf{r}_i \cdot \mathbf{r}_j \rangle = l^2 \delta_{ij}$. Because $\langle \mathbf{r}_i^2 \rangle = l^2$, the obtained formula is:

$$\langle \mathbf{R}_e^2 \rangle = \langle R_e^2 \rangle = N l^2. \tag{3.4}$$

- **Freely rotating chain**: all bond lengths and bond angles ϕ are fixed, but there is a free rotation around single bonds. We define a complementary angle θ (see Fig 3.1) as: $\theta = 180° - \phi$ and express the scalar product of i-th and j-th bond vector by formula for cosine of this angle:

$$\cos \theta_{i,j} = \frac{\mathbf{r}_i \cdot \mathbf{r}_j}{l^2}. \tag{3.5}$$

  When the distance $|j - i|$ between bond vectors i and j increases, their orientations become less correlated, because it is possible to rotate $|j - i|$ single bonds between them. Then the average value of the scalar product of vectors $\langle \mathbf{r}_i \cdot \mathbf{r}_j \rangle$ is a rapidly decaying function of the distance $|j - i|$ along the chain:

$$\langle \mathbf{r}_i \cdot \mathbf{r}_j \rangle = l^2 (\cos \theta)^{|j-i|} \tag{3.6}$$

We substitute the second term on the right side of eq. 3.3 with eq. 3.6 and as a result we get formula for $\langle \mathbf{R}_e^2 \rangle$ of freely rotating chain:

$$\langle \mathbf{R}_e^2 \rangle = \langle R_e^2 \rangle = Nl^2 \frac{1+\cos\theta}{1-\cos\theta}. \tag{3.7}$$

Although there is no free motion of segments as in the case of the freely jointed chain, the interactions at long distances are ignored and therefore this model belongs to the category of ideal chain.

A limiting case of freely rotating chain is a chain with a extremely small bond length, $l \to 0$, and bond angle close to zero, $\theta \to 0$. It is called **worm-like chain**, because it looks like an infinitely thin chain of a continuous curvature. The worm-like chain has a defined value of contour length:

$$R_{\max} = Nl\cos(\theta/2) \tag{3.8}$$

and constant value of persistence length (see chapter 5).

3.2 Coarse-grained chain

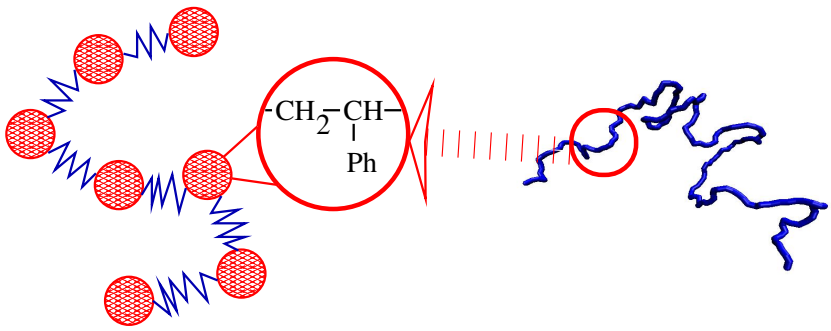

Figure 3.2: Model of coarse-grained chain

In the simulations of polymer solutions, we have to deal with different length scales. Synthetic linear polymer chains are thousands times longer ($\sim 10^3$Å) than one monomeric unit ($\sim 10^0$Å). Detailed atomistic simulation of such a long chain would be extremely time and computationally demanding. Moreover, an exact quantitative description of the system is in many cases unnecessary. Therefore we pass from a fully detailed model to a simpler one. This process is called coarse-graining.

A coarse-grained model of the chain can be created by replacing several atoms and groups by one effective elementary unit of the chain. Some of the physico-chemical details are implemented as a chain stiffness, excluded volume of building blocks or their connectivity, so we don't lose completely the information on the nature of monomeric units. [20] The parts of the coarse-grained chain interact *via* simple effective potential. It allows to simulate multicomponent systems over longer times than in case of simulations with full atomistic details. This representation is used for simulations of real polymers. Because of the simplifying nature of the coarse-grained model, we get only quantitative predictions of polymer properties. [21]

There are two categories of real chain models:

- models of specific polymers: they fit to the particular polymers, the force field and other characteristics of the system have to be predetermined by atomistic simulations.

- generic polymer models: they describe a group of polymers (linear, block copolymers..), the common features of the group are included in model by setting the interactions or volume of building blocks.

In this thesis the second approach is used. The semiflexible polyelectrolytes are simulated on the basis of a bead-spring model. [22] This coarse-grained model is common for simulations of polymers in solution. It is schematically depicted in Fig. 3.2. The modeled chain consists of spherical beads connected by springs. Each bead represents one or more monomeric units, the number of monomeric units per beads depends on a particular problem that we study. The spring is responsible for effective flexible bond, so the value of bond length is not constant and we get only its average. The spring allows the modeling of elastic properties of the chain.

The beads in our simulations have the same size and every bead bears the unit charge (i.e. the chain is positively charged). From now on we refer to "monomeric units" when we speak about the beads forming a chain and "counterions" is a term for beads representing negatively charged ions. Because of the flexible bond between beads, a value of the average bond length $\langle l \rangle$ is used in calculations. To make the notation simpler, we omit the brackets in the thesis and we use the symbol l for the bond length averaged over all equilibrated conformations of the polyelectrolyte (see next section). There are long and short range interactions between beads in the chain and counterions. To restrict the values of bond angles, an angle potential can be implemented. As a result we obtain a bead-spring model with specific stiffness, which takes into account the excluded volume of monomeric units and interactions with solvent.

4. Simulation method

What is not possible in real life it is possible in virtual reality. What is not possible to realize in experiment, can be modeled in molecular simulations. Simulations act as a bridge between theory and experiment. They form an essential part of the research of polymers, because they allow us to calculate polymer properties that can not be measured, thanks to simulations we can investigate the validity of theoretical approaches and they can be used for study in different length and time scales.

This chapter describes the simulation technique that was applied for study of polyelectrolyte solution. It contains a section about interactions between particles and about a model of solvent. In the end some technical details are discussed in order to explain the connection between real and simulated system.

4.1 Introduction to Molecular dynamics

Molecular dynamics is a computer simulation method for studying the time evolution of a many-body system. [5] The system consists of a set of atoms or molecules, or in our case of a polyelectrolyte chain in an implicit solvent (see section 4.3). The particles are localized in the simulation box, the initial configuration is given by positions of particles. The initial velocities are selected arbitrarily and the interaction potential $U(\mathbf{R}^N)$ is implemented (see section 4.2). The motion of particles in the system obeys the Newton's laws

$$m_i \frac{\mathrm{d}^2 \mathbf{R}_i}{\mathrm{d}t^2} = \mathbf{F}_i \qquad i = 0, 1, 2, 3...N, \tag{4.1}$$

where t is a time, $\mathbf{F}_i$ is a force on a particle i with a mass m_i and can be calculated as a gradient of interaction potential:

$$\mathbf{F}_i = -\frac{\partial U(\mathbf{R}_N)}{\partial \mathbf{R}_i}. \tag{4.2}$$

The equations of motion are solved by step-by-step numerical integration. It means that the time is divided into discrete time intervals - time steps Δt and the integration is provided by using a finite difference method. We used the Velocity-Verlet integration scheme. [23] After the integration new coordinates of particles are obtained and the value of time increases to $t + \Delta t$. After particular number of time steps n_s the simulation output is represented by evolution of calculated properties in time. The measurement is performed in simulation as a calculation of time averages of desired quantities A [24]:

$$\langle A \rangle = \frac{1}{n_s} \sum_{i=1}^{n_s} A(i\Delta t). \tag{4.3}$$

In simulations presented in this thesis, the number of particles and the volume V are not changing and therefore their constant values are set in the beginning of simulation. The average value of temperature T is kept constant as well. It is provided by the thermostat (see section 4.3). This choice of invariant quantities corresponds to a canonical ensemble. [24]

4.2 Interaction potential

Not only the model of a chain but also the applied interaction potentials should reflect the real properties of the studied polyelectrolyte solution. They have to describe all forces acting on the particles in the system. However, they should be easy processable, because the calculation of forces (eq. 4.2) is the most time demanding part of the simulation process. Therefore usually only pairwise interactions between beads are considered and the contribution of solvent is treated implicitly.

4.2.1 Short range potentials

Non-bonding potential
For the description of attraction or repulsion between the particles in the system usually the Lennard-Jones potential is used. In our case Lennard-Jones potential was slightly modified, because we use a model of athermal solvent (see below). The attractive part of the potential is omitted and only the repulsive part remains. It was achieved by shifting the potential at the position of its minimum. The final form is known as the Weeks-Chandler-Andersen potential (WCA) [25]:

$$U_{WCA}(r_{ij}) = \begin{cases} 4\epsilon \left[\left(\frac{\sigma}{r_{ij}}\right)^{12} - \left(\frac{\sigma}{r_{ij}}\right)^{6} + \frac{1}{4} \right] & r_{ij} \leq 2^{\frac{1}{6}}\sigma \\ 0 & r_{ij} > 2^{\frac{1}{6}}\sigma \end{cases} \tag{4.4}$$

Parameter ϵ controls the steepness of the interaction potential and σ is a diameter of beads in simulations. The value of parameter ϵ in every simulation in this thesis was chosen to model an athermal solvent.[2] In athermal solvent there are only excluded volume interactions among the particles and beads act like relatively hard spheres when they get closer. The WCA potential with the given parameters is implemented for every bead without exception. Because the beads are the same size, there is no difference in non-bonded interaction of different types of particles (monomer-monomer, monomer-counterion...) and a value of energy calculated from WCA potential is dependent only on distance between beads.

Bonding potential
The beads in the chain are connected by the spring that is modeled via an attractive finitely-extensible non-linear elastic (FENE) potential:

$$U_{\mathrm{FENE}}(r_{ij}) = \begin{cases} -\frac{1}{2} k_{\mathrm{FENE}} R_{\mathrm{FENE}}^2 \ln \left[1 - \left(\frac{r_{ij}}{R_{\mathrm{FENE}}}\right)^2 \right] & r_{ij} < R_{\mathrm{FENE}} \\ \infty & r_{ij} \geq R_{\mathrm{FENE}} \end{cases}, \tag{4.5}$$

with parameters k_{FENE} and R_{FENE}. Parameter R_{FENE} is the maximum stretching of the flexible bond. The values of the parameters chosen for our simulations were relatively high, close to the typical values used for model of polymer networks. This choice

should assure that the chain crossing is impossible and that the fluctuation of bond length is minimal. [26] The values of parameters are summarized in section 4.4.

The combination of FENE potential and WCA potential (eq. 4.4) gives an anharmonic spring interaction with a single minimum. The obtained potential is shown in Figure 4.1.

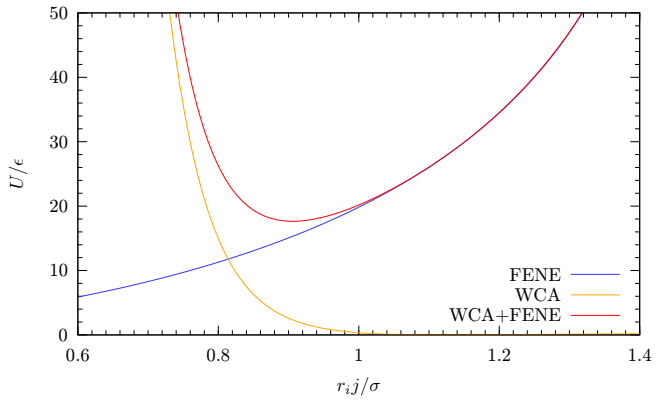

Figure 4.1: FENE and WCA potentials as attractive and repulsive components of the interaction potential

Angle potential
A model of semiflexible chain requires a restriction of flexibility of the chain. The bond angles are not entirely fixed as it was in case of freely rotating chain, but the restriction is done by applying an angle potential. The angle potential belongs to the three-body interactions and it is the only many-body interaction that we used. The selected potential has a harmonic form:

$$U(\phi) = \frac{1}{2} k_{\text{bend}} (\phi - \phi_0)^2, \tag{4.6}$$

where k_{bend} is the bending constant and term $(\phi - \phi_0)$ expresses a fluctuation of bond angle ϕ about the desired equilibrium value ϕ_0. The value of ϕ_0 was set to $\phi_0 = \pi$, which corresponds to completely stretched configuration. This choice of ϕ_0 allows to replace $(\phi - \phi_0)$ on the right side of eq. 4.6 with angle θ (see definition in sec. 3.1).

After the substitution of θ to expression for angle potential the potential will have a form similar to bending potential given by Hook's law for polymers. It is useful, because we get the connection between parameter k_{bend}, that can be set in the beginning of the simulation, and bending of the chain. [2, 27] Generally, if the value of bending constant k_{bend} is high, the value of bond angle tends to be equal to ideal value ϕ_0 and the polymer appears to be stretched. The values of the bending constant were chosen according to assumptions for semiflexible chains (see section 4.4).

4.2.2 Long range potential

In our simulations every monomeric unit bears a unit charge $+e$ and every counterion is charged negatively with charge $-e$. Charged species in system interact via electrostatic long range interactions. In a salt-free solution the pure Coulomb potential is used. When the salt is added to the solution, the screening effect of the ions of salt is taken into account.

Then the potential acting on charged particles doesn't decay like $1/r_{ij}$ but according to Debye-Hückel (DH) theory the potential has a form:

$$U_{\mathrm{DH}}(r_{ij}) = k_B T l_b \frac{e^{-\kappa r_{ij}}}{r_{ij}}, \tag{4.7}$$

where r_{ij} is the distance between the charges, k_B is the Boltzmann constant, κ is a reciprocal value of the Debye screening length and the Bjerrum length l_b expresses the strength of the bare Coulomb electrostatic interaction [3]:

$$l_b = \frac{e^2}{4\pi\varepsilon_r\varepsilon_0 k_B T} \tag{4.8}$$

The ε_r and ε_0 denote in previous equation the relative dielectric constant of the medium (solvent) and the vacuum permittivity. At the distance equal to the Bjerrum length the interaction energy of two unit charges e gets the value of thermal energy $k_B T$. For water at room temperature this distance is $l_b \approx 7.14$Å.

Debye screening length κ^{-1} from equation 4.7 is related to the ionic strength I:

$$\kappa^2 = 4\pi l_b I, \tag{4.9}$$

The electrostatic interaction is screened only at distances larger than Debye screening length. At shorter distances the particles interact *via* unscreened Coulomb potential.

The use of DH theory for description of electrostatic interactions in solutions is limited. The validity of this theory is restricted to the solutions with relatively high ionic strength. If the calculations of properties of polyelectrolytes in salt-free solutions are based on the Debye-Hückel approach, the incorrect values of osmotic pressure or end-to-end distance can be obtained. [28] It is caused by the underestimation of the role of entropy. Moreover, DH theory doesn't account for the counterion condensation (see sec. 4.3), therefore it is not suitable for simulations of strongly charged polyelectrolytes in solutions with relatively high density. The values of κ for our simulations were selected according to the previous considerations: the salt-free regime or solutions with very low ionic strength were omitted, but also the value of κ shouldn't be very high, because then the behaviour of polyelectrolytes in solution is similar to neutral polymers. The values of κ used in our simulations correspond to medium ionic strength, i.e. neither the low salt nor the high salt regimes are studied. They are listed in section 4.4.

4.3 Modeling of the solution

If we wanted to study an explicit effect of solvent molecules on a chain movement in large polyelectrolyte solution, it would take hours of computational time, because the studied system would consist of thousands of particles. Due to this fact the solvent molecules are treated implicitly and the interactions with solvent are usually simulated as random forces, that mimics the random collisions of particles with the surrounding medium. [29] These random forces cause jumps in time evolution of kinetic energy and it leads to warming or cooling of the solution, because the average system temperature T is closely related to kinetic energy:

$$\sum_{i=0}^{N} \frac{m_i |\mathbf{v}_i|^2}{2} = \frac{d}{2} k_B T_k, \tag{4.10}$$

$$\langle T_k \rangle = T.$$

In this equation d denotes the number of degrees of freedom, $\mathbf{v}_i$ is a velocity of $i-$th particle and T_k is so called kinetic temperature.

One possibility, how to control the temperature in canonical simulation and simultaneously model the interactions with a solvent is coupling the system to a heat bath. [30] We use the Langevin thermostat. The implementation of the thermostat is done by modification of the Newton's equations of motion, where two forces are added to the right side of the equation:

$$m_i \frac{\mathrm{d}^2 \mathbf{R}_i}{\mathrm{d}t^2} = \mathbf{F}_i - \Gamma \frac{\mathrm{d}\mathbf{R}_i}{\mathrm{d}t} + \mathbf{F}_i^r(t). \tag{4.11}$$

$\mathbf{F}_i^r(t)$ is the stochastic force that represents the effect of solvent and $\Gamma(\mathrm{d}\mathbf{R}_i/\mathrm{d}t)$ is a drag force, whereas Γ denotes the friction coefficient. These two forces are coupled through the fluctuation-dissipation theorem [19]:

$$\langle \mathbf{F}_i^r(t) \cdot \mathbf{F}_i^r(t') \rangle = 6 k_B T \Gamma \delta_{ij} \delta(t - t'), \tag{4.12}$$

where δ_{ij} is the Kronecker delta and $\delta(t - t')$ the Dirac delta function.

The simulation of salty solution includes also modeling of the added ions. They are taken into account in the simulations only *via* Debye-Hückel potential (eq. 4.7), so they are not explicitly placed in the simulation box. The amount of added salt influences the value of κ, which is proportional to the ionic strength of solution.

On the other hand, the counterions are considered as charged beads with a negative unit charge. They are simulated explicitly, because this work handles solutions of strongly charged polyelectrolytes, where the counterion condensation can occur. [31, 32] It happens when the electrostatic attraction of counterions to the polymer chain is higher than the contribution from their translational entropy in the solution. Because in our simulations the counterions are present in the simulation box, we should be able to observe the condensation directly in simulation snapshots. However, no condensation was observed.

We avoid the counterion condensation also by simulating a dilute system. It contains only one polyelectrolyte chain in simulation box and the box was much longer than average end-to-end distance of polymer.

4.4 Simulation details

The simulations were performed using the simulation software ESPResSo - **E**xtensible **S**imulation **P**ackage for **Re**search on **So**ft Matter [23]. This simulation package was designed by research group from Max-Planck-Institute for Polymer Research in Mainz in Germany for simulations and analysis of coarse-grained models with emphasis on charged systems.

The simulation process is composed of three parts:

- creating of system
- warm-up
- integration loop and analysis

Firstly, the basic components of the system are specified: the number of polymers in the box, their length, fraction of charged monomeric units, interactions and so on. There was only one fully charged polyelectrolyte chain in the simulation box in our simulations. To avoid an effect of the walls of the box on the chain, the periodic boundary conditions were applied. It means, that we replicate the box with particles by translation in all three directions throughout space. As a result our system looks like infinitive lattice created from periodically repeated box. For more information about evaluation of interactions in such a system see [24]. The fundamental characteristics of our system under investigation are listed in the next table:

Table 4.1: Characteristics of the system

quantity	symbol	reduced unit	value
number of monomeric units per chain	N_m		200
fraction of charged monomeric units	f		1
number density of particles	ρ	σ^{-3}	2.10^{-5}
bond length	l	σ	$\approx$1.0
friction coefficient	Γ	$\sigma^{-1}\sqrt{k_BT/m}$	1.0

The quantities are given in typical units for simulations called reduced units. It prevents from dealing with too small or too big numbers in calculations. For example, if the majority of measured lengths in simulation have the same order of magnitude, it is convenient to define a basic unit as one of the constant lengths (as diameter of beads, Bjerrum length...) and express all other quantities as its multiplies. The energy scale in this work is given by setting $k_BT = 1$. The second basic unit is mass of the bead $m = 1$. The length scale is set by the diameter of beads $\sigma = 1$.

The initial random configuration created in the first part of the simulation can include overlapping beads. Therefore we start a warm-up loop to reorganize the particles in the system, so that the separation between the beads was as big as we require. It is done by applying the pure repulsive WCA potential. The potential is modified in order to slightly change the conformation, so called "force cap" is used. [23] It means that for distance below the particle size force doesn't become extremely large, but is "capped" to the given value. This value is increasing during the warm-up loop and so the overlapping of particles is getting unfavourable. When the given minimum distance between beads is reached, the warm-up loop is stopped and force cap is switched off.

The interaction potentials described in sec. 4.2 are firstly introduced in simulation in the third part before integration. The parameters chosen for our simulations are summarized in the table:

Table 4.2: Interaction parameters

quantity	symbol	reduced unit	value
steepness of WCA potential	ϵ	k_BT	0.34
WCA cut-off distance	r_{cut}	σ	$2^{\frac{1}{6}}$
spring constant	k_{FENE}	k_BT/σ^2	30.0
maximum bond stretching	R_{FENE}	σ	1.5
bending constant	k_{bend}	k_BT	8.0-40.0
inverse Debye screening length	κ	σ^{-1}	0.04-0.07

The equations of motion are then integrated with time step Δt=$0.01\sigma\sqrt{m/k_BT}$. The analysis of data begins after equilibration of the system. System is equilibrated when its total energy fluctuates around average constant value. The equilibration time was established from the time evolution of energy and equals to 2×10^7 time steps. Overall time of simulation was 44×10^7 time steps.

5. Persistence length

5.1 Definition of persistence length

The persistence length l_p is a measure of flexibility of a polymer chain. It can be defined as a distance over which the correlation in orientation of the chain segments is lost. So at distances shorter than the persistence length the chain remembers the direction of the previous segments and the orientation of segments is correlated. It means that the higher is the value of persistence length, the stiffer is the chain and its bending is more difficult.

If the value of persistence length is higher than length of the chain, the chain behaves like a stiff rod. The values of persistence length close to the bond length are typical for flexible chains, their segments move freely without any restriction and their bending doesn't require a large applied force. The focus of my study is somewhere in between these two limiting cases and involves the characterization of persistence length of semiflexible polymers.

The concept of the persistence length is quite intuitive but the description of the orientation correlation of the chain segments can be done by many different ways. Therefore there exist several equations for the calculation of persistence length. Some of the most common definitions are summarized here:

1. *The average projection of the end-to-end vector on the tangent to the chain contour at a chain end.* [33]
   If the chain is modeled as a set of bond vectors, then the tangent to the chain contour at the chain end can be represented by the first bond vector. We use the eq. 3.2 and obtain:
   $$l_p = \frac{1}{|\mathbf{r}_1|} \langle \mathbf{R}_e \cdot \mathbf{r}_1 \rangle = \frac{1}{l} \sum_{i=1}^{N} \langle \mathbf{r}_1 \cdot \mathbf{r}_i \rangle = l \sum_{i=1}^{N} \langle \cos \theta_{1,i} \rangle \,. \tag{5.1}$$
   The angular brackets $\langle .. \rangle$ stand for the average over all possible conformations of chain with proper statistical weights. This definition doesn't take into account the end-effects that can be observed even for neutral polymers, so its use would be justified only in an ideal case of an infinitely long chain that can not be achieved in simulations.

2. *The average projection of the end-to-end vector on any bond vector along the chain.* [34]
   $$l_p(k) = \frac{1}{|\mathbf{r}_k|} \langle \mathbf{R}_e \cdot \mathbf{r}_k \rangle = \frac{1}{l} \sum_{i=1}^{N} \langle \mathbf{r}_k \cdot \mathbf{r}_i \rangle \,. \tag{5.2}$$
   Symbol k denotes position on the chain. This definition allows to define the persistence length locally and avoid the problems with the end effects.

3. *The decay contour length of angular correlations.* [2]
   As it was explained in sec. 3.1, the correlation of orientations of bond vectors becomes insignificant with increasing distance between them. The correlation function can be expressed by a scalar product of bond vectors separated by distance j. For neutral polymers the correlation function decays exponentially and the value of persistence length can be obtained from its single exponential fit:

$$\frac{\langle \mathbf{r}_i \cdot \mathbf{r}_{i+j} \rangle}{l^2} = \langle \cos\theta_{i,i+j} \rangle = \exp\left(-\frac{jl}{l_p}\right). \tag{5.3}$$

   The orientational correlation function (OCF) of polyelectrolytes doesn't follow the single exponential decay and expression for average value of cosine $\langle \cos\theta_{i,i+j} \rangle$ is much more complicated (see section 5.2).

4. *Integral of the orientational correlation function* [35]

$$l_p = \int_0^{R_{\max}} \langle \cos\theta(s) \rangle \, \mathrm{d}s. \tag{5.4}$$

   The definition was derived for a continuous-chain model (see section 3.1) and s is a distance along the chain contour. The orientational correlation function is integrated over space curve with length $R_{\max}$.

5. *Parameter that specifies the bending energy of the chain.* [6]
   We assume a model of a continuous chain. The elastic bending energy per unit length of the chain is equal to:

$$\Delta E_{\mathrm{bend}} = \frac{1}{2}\kappa_b \left(\frac{1}{\mathrm{R}_c}\right)^2, \tag{5.5}$$

   where R_c is a radius of curvature and and κ_b is the bending modulus of polymer.
   If there is no other contribution to the bending of polymer (as for example from electrostatic repulsion of charged parts of the chain) then the ratio of bending modulus and thermal energy k_BT define the bare (intrinsic) persistence length of the chain:

$$l_p^0 = \frac{\kappa_b}{k_BT}. \tag{5.6}$$

   It can be shown that for a semiflexible neutral polymer whose bending is described by angle potential (eq 4.6), the bending modulus is identical with the bending constant κ_b=k_{bend}. [36]

Under special conditions some of the mentioned definitions are equal.
For instance, the first definition can be obtained from second one when we set $k = 1$.
When we consider a long continuous chain with length $R_{\max}$ and with single exponential decay of orientational correlation function:

$$\langle \cos\theta(s) \rangle = \exp\left(-\frac{s}{l_p}\right),$$

then the integral of the orientational correlation function results in

$$l_p = \int_0^{R_{\max}} \langle \cos\theta(s) \rangle \, \mathrm{d}s = \int_0^{R_{\max}} \exp\left(-\frac{s}{l_p}\right) \mathrm{d}s = l_p\left(1 - \exp\left(-\frac{R_{\max}}{l_p}\right)\right) \cong l_p.$$

So we get the same value of persistence length either from the fit or from the integration of orientational correlation function.

5.2 Theories of the persistence length of polyelectrolytes

The definitions 2.-5. from previous section (eq. 5.2-5.6) can be applied for neutral polymers and there will be no significant differences between them. In case of polyelectrolytes we have to deal with different length scales and an additional theory involving electrostatic interactions is necessary. The electrostatic interactions are treated at the level of the Debye-Hückel approximation. Salt-free solution and polyelectrolytes interacting *via* pure Coulomb potential were discussed in my bachelor thesis. [36]

The most famous theory on the bending of PEs is the Odijk, Skolnick, Fixman (OSF) theory. [8, 9] It was derived for stiff charged worm-like polymers. The configuration of a straight rod was taken as a reference state. It was assumed that there are two contributions affecting the stiffness of polyelectrolytes-the intrinsic l_p^0 and electrostatic l_p^e persistence length. According to OSF approach, they are additive and their sum is the total persistence length l_p^t:

$$l_p^t = l_p^0 + l_p^e \tag{5.7}$$

The value of the electrostatic persistence length was obtained from the calculation of the difference between the bending energy (eq. 5.5) of a considered continuous chain and the reference state. The changes in bending energy are caused by the electrostatic repulsion. The final formula for the electrostatic persistence length is:

$$l_p^e = \frac{f^2 l_b}{4\kappa^2 l^2} \tag{5.8}$$

The OSF approach was discussed recently in a number of articles, which presented results from simulations (e.g. [14, 37, 38]) and variational methods (e.g. [27, 39]). They were focused mainly on the κ-dependence of l_p^e. It was found out, that the OSF theory is not valid for flexible chains, which have the value of l_p^e proportional to κ^{-1}.

In simulations the persistence length is calculated usually from the orientational correlation function. It was observed in the studies of semiflexible [14] and flexible chains [40], that there is no single exponential decay of OCF as is predicted by a concept of one total persistence length. Data shows, that the chain stiffness differs at two distinct length scales. The first studies of this phenomenon just described the different behaviour of OCF and they fitted only the part of the OCF pertaining to long distances between the bond vectors in order to obtain the value of l_p^e. [37] It was motivated by the fact, that the electrostatic contribution to the chain rigidity was supposed to be important at the large length scales.

The predictions of the different behaviour of the chain stiffness at different length scales led to the progress in variational approaches and resulted in definition of crossover length s_c [39]:

$$s_c = \frac{(l_p^0)^{1/2}}{\kappa (l_p^0 + l_p^e)^{1/2}}. \tag{5.9}$$

The crossover length is a contour length of the chain at which the contributions to chain bending energy from intrinsic stiffness and from electrostatic interactions are comparable. For distances j between the bond vectors $j < s_c$ the bending of chain is governed by its intrinsic persistence length and at distances $j > s_c$ the additional contribution of electrostatic persistence length becomes significant.

This two scales behaviour can be described according to Manghi and Netz [15] by two limiting expressions for the orientational correlation function:

$$\frac{\langle \mathbf{r}_i \cdot \mathbf{r}_{i+j} \rangle}{l^2} = \begin{cases} 1 - \frac{j}{l_p^0} & j < s_c \\ \exp\left(\frac{-j}{l_p^0 + l_p^e}\right) & j > s_c \end{cases} \tag{5.10}$$

The previous equations were derived for strongly charged polymers $l_p^0 l_b f^2 > 1$ at small screening $l_p^0 l_b f^2 > (l_p^0 \kappa)^2$. Manghi and Netz assumed the double exponential decay of OCF and they postulated that OCF should be equal to $1 - \frac{j}{l_p^0}$ for small distances between bond vectors. A condition of continuity of wanted OCF and fulfillment of $\langle \cos \theta_{i,i} \rangle$=1 were the basic requirements for the derivation of formula for orientational correlation function of polyelectrolytes:

$$\langle \cos \theta_{i,i+j} \rangle = B \exp\left(-\frac{j}{l_p^0 + l_p^e}\right) + (1 - B) \exp\left(-j \frac{l_p^e + (1 - B) l_p^0}{l_p^0 (l_p^e + l_p^0)(1 - B)}\right). \tag{5.11}$$

Parameter B can be determined from the assumption that for $j = s_c$ the two limiting cases from eq 5.10 are comparable, so they differ only in constant. We get:

$$B = \exp\left(\frac{-s_c l_p^e}{l_p^0 (l_p^0 + l_p^e)}\right). \tag{5.12}$$

The predictions of Manghi and Netz were based on variational theory for polyelectrolytes and were never proved in simulations.

The double exponential decay of OCF was described also by Gubarev, Carillo and Dobrynin. [16] They acquired it from simulations of semiflexible polyelectrolytes and specified the form of OCF and parameters by using the variational theory. It led to expression:

$$\langle \cos \theta_{i,i+j} \rangle = (1 - \beta) \exp\left(-\frac{j}{\lambda_1}\right) + \beta \exp\left(-\frac{j}{\lambda_2}\right), \tag{5.13}$$

where parameter λ_1 corresponds to total persistence length introduced in OSF theory (eq. 5.7) and λ_2 is defined at low salt concentrations as:

$$\lambda_2 = \left(-\frac{l_p^0 l}{l_b f^2 \ln(l\kappa)}\right)^{1/2}. \tag{5.14}$$

The formula for β can be obtained after some modifications of eq. 5.12. It is apparent, that these two theories are not identical, although they both describe the existence of two length scales in the orientational correlation function. For instance, the second term in eq. 5.11 was chosen in agreement with mentioned conditions whereas the second term in eq. 5.13 and parameter λ_2 has a form characteristic of a semiflexible chain under tension. [27] Moreover, the form of OCF as was designed by Dobrynin and Gubarev can bring difficulties by fitting, because the value of λ_2 is very small at higher salt concentrations.

The concept of the scale-dependent electrostatic persistence length is still under investigation and there is no unique method for determination of l_p^0 and l_p^e from OCF.

5.3 Measurement of the persistence length

The persistence length can be measured only indirectly. An usual way is to measure the end-to-end distance or the radius of gyration and then calculate the persistence length from the relation between R_e or R_g and orientational correlation function (see eq. 3.3). In order to formulate the equation for $\langle \mathbf{R}_e^2 \rangle$ properly, it would be necessary to substitute the $\langle \mathbf{r}_i \cdot \mathbf{r}_j \rangle$ in eq. 3.3 by a double exponential correlation function. However, the most common way is to use a single exponential OCF, simplify the obtained expression and denote the persistence length l'_p in equation as "apparent" [13]:

$$\langle \mathbf{R}_e^2 \rangle = 2l'_p R_{\max} - 2{l'_p}^2 \left(1 - \exp\left(-\frac{R_{\max}}{l'_p}\right)\right) \tag{5.15}$$

This expression was obtained by considering a worm-like chain model. Some corrections to this equation were done in recent years, that take into account for example the excluded volume. [45] Because the experimental method as light scattering or small angle neutron scattering are not able to measure at two length scales, the value of l_p^0 can be obtained from measurement of polyelectrolyte in solution with high ionic strength. [12]

6. Results

6.1 Analysis of data

Time-dependent autocorrelation function of end-to-end distances
During the simulations we get a sequence of configurations by small integration steps, which means that the two successive configurations differ only little. At each integration step we calculate current values of desired properties from the coordinates of particles in a new configuration. Because the conformations are statistically correlated at short timescales, there is no point saving data very frequently. Firstly we estimate the frequency of saving, we run the simulation and save n_c configurations. Then we use the autocorrelation function $C(c)$ to establish the number of time steps, after which we obtain uncorrelated quantities. In our simulations we calculated the autocorrelation function of end-to-end distance:

$$C(c) = \frac{1}{(n_c - c)} \frac{\sum_{i=1}^{n_c - c} (\mathbf{R}_{e,(i)} - \langle \mathbf{R}_e \rangle)(\mathbf{R}_{e,(i+c)} - \langle \mathbf{R}_e \rangle)}{\langle \mathbf{R}_e^2 \rangle - \langle \mathbf{R}_e \rangle^2}. \tag{6.1}$$

Brackets $\langle .. \rangle$ denote the average over the whole simulation, vectors $\mathbf{R}_{e,(i)}$ and $\mathbf{R}_{e,(i+c)}$ are the end-to-end distances of i-th and $(i+c)$-th saved configuration. The value of c lay in the interval from 0 to 200, the final value of n_c was equal to 2200, so the time interval between two following saved configurations is represented by $44 \times 10^7/2200 = 2 \times 10^5$ time steps. The initial part for $c < 70$ of typical autocorrelation function shape is plotted in Fig. 6.1.

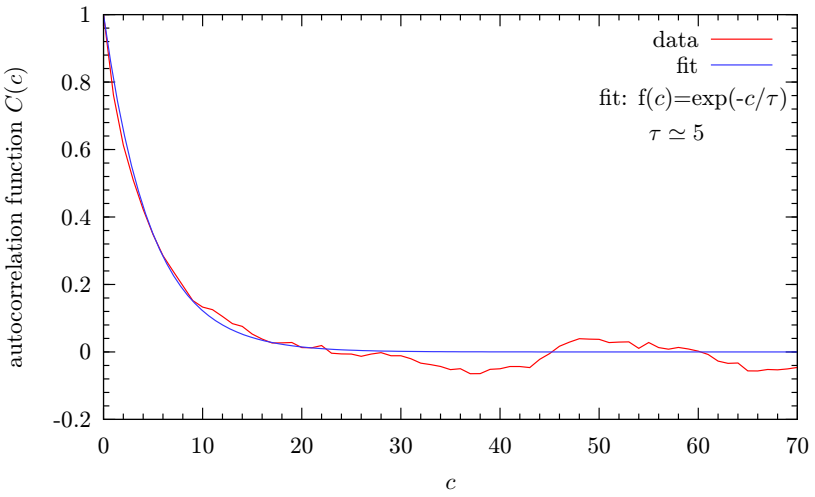

Figure 6.1: Initial part of autocorrelation function of end-to-end-distance of PE with k_{bend}=20.0 and κ=0.05

As we can see, for small values of c the correlation function can be fitted by a single exponential function and then for cca. $c > 25$, it fluctuates around zero. We didn't plot the evolution of autocorrelation function for the whole interval of c (from 0 to 200), because we are interested in the initial decay and the data for higher values of c show only the fluctuations.

We used a function: f(c)=exp($-c/\tau$) for fitting the first part of the autocorrelation function ($c < 25$). Parameter τ obtained from the fit gives the value of c for which the autocorrelation function equals e^{-1}. For the polyelectrolyte chain with characteristics k_{bend}=20.0 and κ=0.05, we get $\tau \doteq 5$ from the fit. The value of τ is very similar for all studied polyelectrolyte systems. It tells us, that there is insignificant correlation between the end-to-end distances calculated from every fifth saved configuration. So from the total number of saved configurations n_c there are n_c/τ=440 of them statistically independent. This number of statistically independent conformations is sufficient, because to the orientational correlation function of bonds vectors, which is used in our study of persistence length, each conformation contributes by 3-10 uncorrelated values.

End effects

As it was discussed in section 5.1 the second definition of the persistence length is applicable for any part of the chain. When we determine the value of persistence length according to the second definition (eq. 5.2), e.g. as the average projection of the end-to-end vector on k-th bond vector, we are able to study the dependence of its value on the position on the chain, k. The results for the polyelectrolyte with k_{bend}=8.0 in solutions with different ionic strength are presented in Fig. 6.2. The persistence length $l_p(k)$ of a neutral polymer is also depicted for comparison.

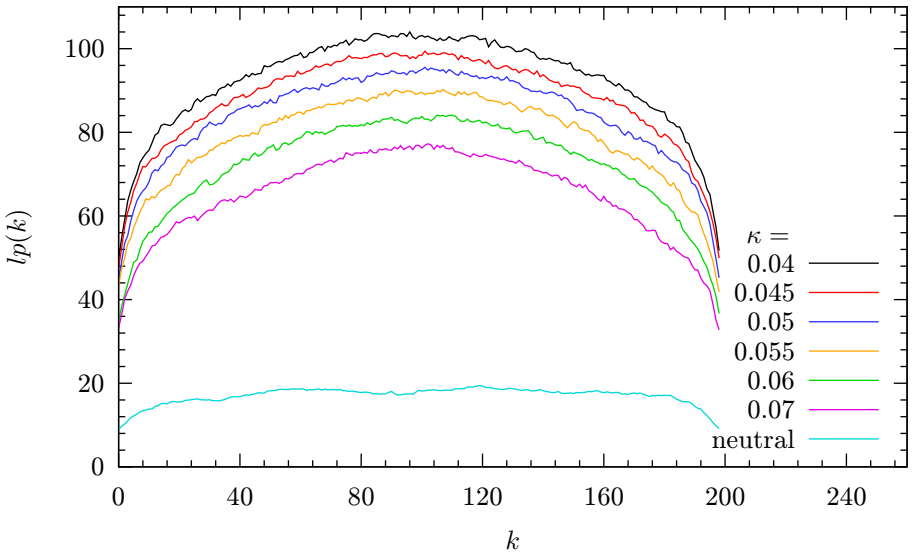

Figure 6.2: Local persistence length according to eq.5.2 for PE with k_{bend}=8.0 as a function of position on the chain k

The persistence length defined by equation 5.2 corresponds to the local persistence length, because its value is strongly influenced by the position on the chain. The $l_p(k)$ is smaller near the chain ends and increases towards the interior part of the chain where it is almost constant. It is a consequence of end effects, that can be observed also in case of

neutral polymers (see Fig. 6.2). The end effects are important when the chain has a finite length. In the case of polyelectrolytes the different behaviour at the chain ends is caused especially by asymmetric electric field around charged monomeric units located close to the ends. In the interior region of the chain the charged monomeric units are surrounded by charged species and their distribution is uniform, whereas at the ends the situation is different.

When we want to eliminate end effects in our calculations we have to determine the persistence length only from the region of the chain, where the properties of the chain are constant. We identified the constant region as a middle part of chain with length of 100 monomeric units, so we omitted the 50 monomeric units at every end from the further analysis of l_p. We found that the exclusion of 50 units is sufficient for all studied systems.

As it is shown in this section, the value of the persistence length can be strongly influenced by the end effects and therefore it is not reasonable to determine the persistence length according to eq. 5.1. In the case of a neutral polymer, the second definition serves for estimation the value of intrinsic persistence length. [34] The value of intrinsic persistence length is given by the value of $l_p(k)$ at which we are able to observe a plateau in $l_p(k)$ curve. But this approach can not be applied for polyelectrolytes, because the basic assumption of one persistence length is not valid when the polymer chain is charged.

6.2 Determination of the persistence length

Statistical treatment of data
After the equilibration of a system, we started to collect data for evaluation of the persistence length. The time of simulation t_s, that we used for evaluation of the desired quantities, was splitted into five equal time intervals $t_1 = t_2 = t_3 = t_4 = t_5 = t_s/5$ (see in Fig. 6.3).

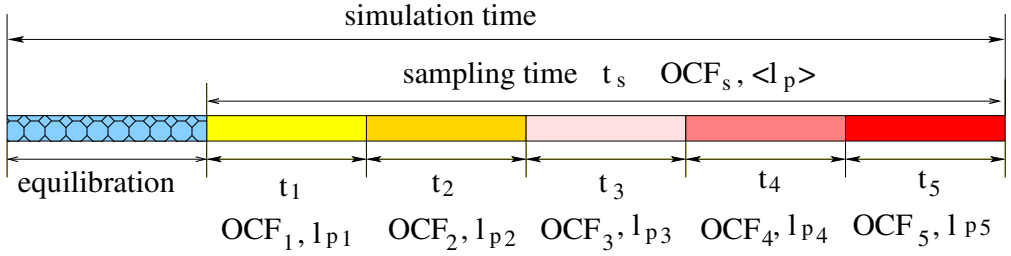

Figure 6.3: The division of the simulation time

The persistence length was determined from the orientational correlation function, that was defined by eq. 5.3:

$$\frac{\langle \mathbf{r}_i \cdot \mathbf{r}_{i+j} \rangle}{l^2} = \langle \cos \theta_{i,i+j} \rangle \,. \tag{6.2}$$

For every time interval we calculated the average normalized scalar product of bond vectors as a function of distance between them, thus we got five orientational correlation functions (in Fig. 6.3 labeled as OCF_1-OCF_5) and five persistence lengths generally denoted as l_{p1}-l_{p5}. The persistence length obtained from the whole sampling interval was considered as the main value of persistence length $\langle l_p \rangle$. This procedure allowed us to

estimate the error of persistence length as:

$$\sigma_{l_p} = \sqrt{\frac{1}{4}\sum_{i=1}^{5}(l_{p,i} - \langle l_p \rangle)^2}. \tag{6.3}$$

As was explained in the previous section, only the region in the middle of the chain was used for calculation of the OCF, which corresponds to set of bond vectors $\{\mathbf{r}_i\}$=($\mathbf{r}_{51}$...$\mathbf{r}_{150}$). To improve the statistics of averaging, the pair of bond vectors $\mathbf{r}_i$ and $\mathbf{r}_{i+j}$ moved along the selected region of the chain, such that the index i increased its value by one and the distance j kept constant. Firstly the scalar products for given configuration were divided by the number, that says how many times per region we calculated the scalar product for fixed j. By this method we obtain one averaged OCF for every saved configuration. Finally, we averaged the orientational correlation functions in order to get one OCF for selected time intervals (OCF_1-OCF_5).

Double exponential decay of OCF

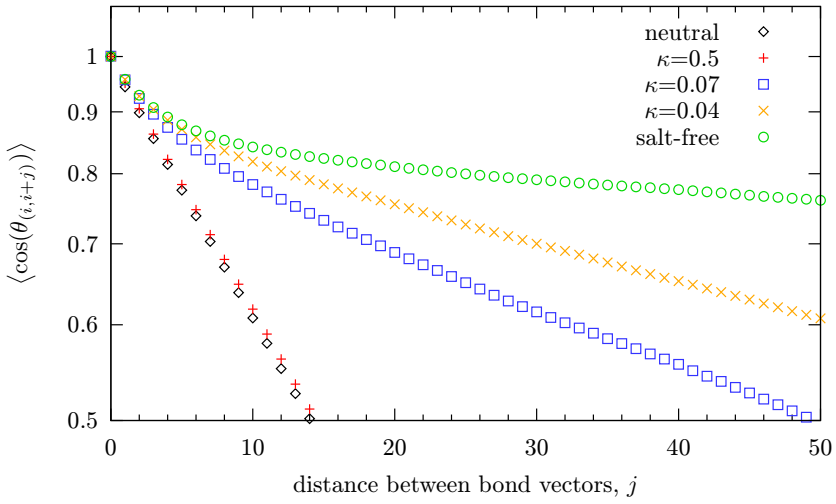

Figure 6.4: The OCF for chains with the same intrinsic stiffness k_{bend}=20.0 under various conditions.

In Fig. 6.4 the correlation functions OCF_s of polyelectrolytes with the same intrinsic stiffness (k_{bend}=20.0) are plotted. The polyelectrolyte solutions have different ionic strength. There are two limiting cases: polyelectrolyte in salt-free solution and polyelectrolyte in solution with high ionic strength (κ=0.5). In order to see the difference between single and double exponential decay of OCF, we focused on the initial part of OCF ($j < 50$) and we also plotted the orientational correlation function of a neutral polymer in water in a semi-logarithmic plot (a linear function). It is obvious, that only the OCF of polyelectrolyte in highly salted solution is a single exponential function of the distance between the bond vectors. In this case, the screening of ions is so strong that the electrostatic repulsion of charged monomeric units along the chain has almost no effect on the chain stiffness and the polyelectrolyte chain behaves similar to a neutral one. In the range of small screening, that we are interested in, the orientational correlation function exhibits the double exponential decay. We can observe the same trend for other studied semiflexible polyelectrolytes (the value of k_{bend} from 8.0 to 40.0).

Table 6.1: The crossover length s_c, intrinsic l_p^0 and electrostatic l_p^e persistence length obtained from the fit according to Manghi and Netz [15] (eq. 4.11) and Gubarev, Carrillo and Dobrynin [16] (eq. 5.13)

		fit: equation 5.11		
k_{bend}	κ	s_c	l_p^0	l_p^e
8.0	0.04	2.1 ± 0.1	9.3 ± 0.2	119.1 ± 7.8
8.0	0.045	2.1 ± 0.0	9.1 ± 0.1	101.1 ± 3.3
8.0	0.05	2.1 ± 0.1	9.1 ± 0.2	89.3 ± 7.0
8.0	0.055	2.0 ± 0.2	8.9 ± 0.3	74.6 ± 10.7
8.0	0.06	2.0 ± 0.1	8.9 ± 0.2	64.9 ± 6.7
8.0	0.07	2.0 ± 0.1	9.0 ± 0.2	52.0 ± 5.6
10.0	0.04	2.3 ± 0.0	11.1 ± 0.1	115.3 ± 5.6
10.0	0.045	2.4 ± 0.1	11.2 ± 0.2	101.3 ± 7.2
10.0	0.05	2.4 ± 0.1	11.2 ± 0.2	83.8 ± 6.6
10.0	0.055	2.4 ± 0.2	11.1 ± 0.3	76.0 ± 11.8
10.0	0.06	2.3 ± 0.1	11.0 ± 0.2	64.5 ± 4.3
10.0	0.065	2.3 ± 0.2	10.8 ± 0.4	57.9 ± 5.1
10.0	0.07	2.2 ± 0.4	10.7 ± 0.4	52.9 ± 11.4
16.0	0.04	2.8 ± 0.2	17.0 ± 0.4	107.9 ± 9.7
16.0	0.045	2.8 ± 0.3	16.7 ± 0.5	91.5 ± 10.6
16.0	0.05	2.7 ± 0.2	16.7 ± 0.3	76.2 ± 7.4
16.0	0.055	2.9 ± 0.1	17.0 ± 0.3	72.8 ± 2.0
16.0	0.06	2.6 ± 0.1	16.4 ± 0.3	55.9 ± 3.4
16.0	0.065	2.7 ± 0.3	16.5 ± 0.4	52.8 ± 6.5
16.0	0.07	2.5 ± 0.3	16.4 ± 0.4	43.8 ± 12.1
20.0	0.04	3.3 ± 0.2	21.4 ± 0.5	112.0 ± 8.4
20.0	0.045	3.0 ± 0.5	20.6 ± 0.6	86.0 ± 19.6
20.0	0.05	3.0 ± 0.4	20.4 ± 0.5	74.1 ± 11.7
20.0	0.055	3.1 ± 0.1	20.7 ± 0.7	67.5 ± 3.4
20.0	0.06	3.1 ± 0.4	20.5 ± 0.6	57.7 ± 8.3
20.0	0.065	2.8 ± 0.4	20.1 ± 0.4	49.7 ± 4.7
20.0	0.07	3.0 ± 0.8	20.5 ± 0.9	45.5 ± 11.9
24.0	0.04	3.2 ± 0.2	24.2 ± 0.4	97.8 ± 10.1
24.0	0.05	3.1 ± 0.1	24.1 ± 0.2	71.2 ± 2.6
24.0	0.055	2.9 ± 0.2	23.6 ± 0.4	63.9 ± 5.6
24.0	0.06	3.0 ± 0.8	23.9 ± 1.0	53.9 ± 14.9
24.0	0.065	2.8 ± 0.3	23.5 ± 0.9	47.9 ± 16.1
24.0	0.07	2.9 ± 0.7	23.9 ± 0.9	43.8 ± 8.4
32.0	0.04	3.6 ± 0.5	31.9 ± 0.8	99.9 ± 16.9
32.0	0.05	3.4 ± 0.5	31.2 ± 1.1	73.9 ± 7.8
32.0	0.055	3.7 ± 0.8	32.3 ± 1.0	64.3 ± 8.1
32.0	0.06	2.9 ± 0.7	30.9 ± 1.4	49.5 ± 10.0
32.0	0.065	3.0 ± 0.9	31.0 ± 1.1	43.3 ± 9.2
32.0	0.07	2.8 ± 1.5	30.7 ± 1.9	39.1 ± 14.1
40.0	0.04	3.5 ± 0.5	38.4 ± 1.0	90.0 ± 15.8
40.0	0.05	3.5 ± 1.0	38.6 ± 1.7	66.5 ± 12.7
40.0	0.055	3.2 ± 1.1	38.0 ± 1.8	58.3 ± 15.5
40.0	0.06	3.0 ± 0.8	37.7 ± 1.4	48.1 ± 9.2
40.0	0.065	3.1 ± 2.0	37.9 ± 3.0	44.3 ± 10.6
40.0	0.07	3.3 ± 1.5	38.4 ± 2.1	41.8 ± 11.3

		fit: equation 5.13			
k_{bend}	κ	λ_1	λ_2	l_p^0	l_p^e
24.0	0.04	122.0	2.9	30.8 ± 4.0	91.3 ± 7.3
24.0	0.05	95.3	2.9	27.1 ± 5.4	68.2 ± 3.2
24.0	0.055	87.5	2.7	22.9 ± 3.5	64.6 ± 5.9
24.0	0.06	77.9	2.8	23.9 ± 11.2	54.1 ± 5.8
24.0	0.065	71.4	2.6	19.9 ± 4.7	51.6 ± 13.9
24.0	0.07	67.7	2.7	21.1 ± 9.7	46.6 ± 2.8
32.0	0.04	131.8	3.4	41.0 ± 11.0	90.9 ± 6.6
32.0	0.05	105.1	3.2	33.4 ± 9.5	71.7 ± 3.3
32.0	0.055	96.6	3.5	38.6 ± 13.8	58.0 ± 5.7
32.0	0.06	80.4	2.7	23.0 ± 10.5	57.4 ± 2.9
32.0	0.065	74.3	2.8	23.5 ± 14.1	50.8 ± 4.3
32.0	0.07	69.8	2.6	19.8 ± 26.6	50.0 ± 10.9
40.0	0.04	128.4	3.3	38.6 ± 11.2	89.8 ± 6.2
40.0	0.05	105.1	3.3	35.6 ± 20.9	69.5 ± 7.3
40.0	0.055	96.3	3.0	29.7 ± 22.6	66.6 ± 6.3
40.0	0.06	85.7	2.8	24.5 ± 14.5	61.2 ± 4.3
40.0	0.065	82.2	2.9	26.4 ± 40.2	55.8 ± 27.9
40.0	0.07	80.3	3.1	28.1 ± 30.0	52.2 ± 17.0

Comparison of theories

Our data are in agreement with the predictions of variational approaches [15, 16].

The systems studied in [15, 16] were similar to ours, they consisted of the semiflexible polyelectrolytes or highly charged chains under small screening (for more information see section 5.2). The form of the orientational correlation function derived by Manghi and Netz is suitable for fitting our simulation data. The substitution of B (eq. 5.12) in equation 5.11 results in a function of three parameters: crossover distance s_c, intrinsic persistence length l_p^0 and electrostatic persistence length l_p^e. We fitted our data by the final form of this expression. The results from the fit are summarized in Tab. 6.1.

We attempted to prove the predictions of Gubarev, Carrillo and Dobrynin [16] as well. The authors combined the results of the simulations with the variational approach. They used a double exponential function described in section 5.2 (eq. 5.13) for a fit of the OCF from simulation data. The relation of the obtained parameters λ_1 and λ_2 to the persistence length of a polyelectrolyte was explained on the basis of the results of the variational method. Our analysis was done in the same way. Firstly, we fitted the simulation data with the function of three parameters (λ_1, λ_2, β) given by eq. 5.13. Then following the procedure of Gubarev, Carrillo and Dobrynin, we expressed the persistence lengths l_p^0 and l_p^e from the formulas for λ_1 and λ_2 (eq. 5.14 and 5.7) from the variational calculations:

$$l_p^0 = \lambda_2^2 \left(-\frac{l_b f^2 \ln(l\kappa)}{l} \right), \tag{6.4}$$

$$l_p^e = \lambda_1 - l_p^0. \tag{6.5}$$

The article of Gubarev, Carrillo and Dobrynin concerned semiflexible polyelectrolytes with $k_{bend} \geq 25.0$, so in order to reproduce their approach, we analyzed the data only from simulations of polyelectrolytes with bending constants 24.0, 32.0 and 40.0. The obtained values of fitted parameters and calculated persistence lengths are listed in Tab. 6.1.

It is obvious, that the accuracy of the estimation of both persistence lengths is strongly limited by the range of applicability of eq. 6.4. If the formula for λ_2 is not valid for our system and the value of l_p^0 is incorrect, the value of l_p^e calculated afterward is wrong as well. Expression 5.14 (and consequently 6.4) is considered to be valid for polyelectrolyte solutions characterized by small values of κ (low salt concentration). When we compare the values of l_p^0 and k_{bend}, that should be equal for our simulation model (see eq. 5.6), we see, that for k_{bend}=24.0 the quantity l_p^0 is within the error comparable with k_{bend} for every value of κ, but for k_{bend}=32.0 and k_{bend}=40.0 there are very high values of standard deviations, in some cases ($\kappa > 0.06$) even higher than main value of intrinsic persistence length. So when the parameter λ_2 is defined by eq. 5.14, we are not able to get reasonable values of l_p^0 nor l_p^e (because of l_p^e and l_p^0 are connected by relation 6.5).

Our analysis based on the approach of Manghi and Netz gives the values of intrinsic persistence length very closed to the values of bending constants. This result is in agreement with our assumptions and with previous studies and theory. [27, 36]

Both theories consider a double exponential decay of the orientational correlation function of polyelectrolytes. The first term in both expressions for OCF (eq. 5.11 and 5.13) describes the behaviour of OCF at long scales. So, one would expect that the parameters λ_1 and $l_p^0 + l_p^e$ are equal. We can see from the results in Tab. 6.1, that this assumption is true. Apparently, there is no difference in the behaviour of OCF at long distances predicted by these two approaches.

The equations eq. 5.11 and 5.13 differ in the expression of OCF for small values of distances between bond vectors. We show that the function derived by Manghi and Netz

allows a good description of correlations at short length scales. If $j \to 0$ we can use the approximation $\exp(-f(j)) = 1 - f(j)$ and we get:

$$\langle \cos\theta_{i,i+j} \rangle = B\left(1 - \frac{j}{l_p^0 + l_p^e}\right) + (1-B)\left(1 - j\frac{l_p^e + (1-B)l_p^0}{l_p^0(l_p^e + l_p^0)(1-B)}\right) = 1 - \frac{j}{l_p^0}. \qquad (6.6)$$

Thus the correlations at short length scales (smaller than crossover length) are expressed as a function of the intrinsic length only as was predicted several years ago. [39] It can be seen also in Fig. 6.4 that our simulation data show the same trend. The initial part of the orientational correlation functions of polyelectrolytes with the same intrinsic stiffness does not depend on the ionic strength of solution. When we examine the expression derived by Gubarev, Carrillo and Dobrynin (eq. 5.13), we find, that the orientational correlation function for small distances between bond vectors depends not only on l_p^0 but also on κ (because $\lambda_2 \sim \ln(l\kappa)$). It means, that the correlations of bond vectors at short distances are influenced by ionic strength of solution. This fact seems to be a reason of disagreement of the theories of Manghi, Netz and Gubarev, Carrillo and Dobrynin.

Due to the above mentioned reasons we concluded that the approach of Manghi and Netz is more appropriate for the semiflexible polyelectrolyte systems. The next step was a more detailed analysis of parameters obtained from the fit: intrinsic l_p^0 and electrostatic l_p^e persistence length and crossover length s_c.

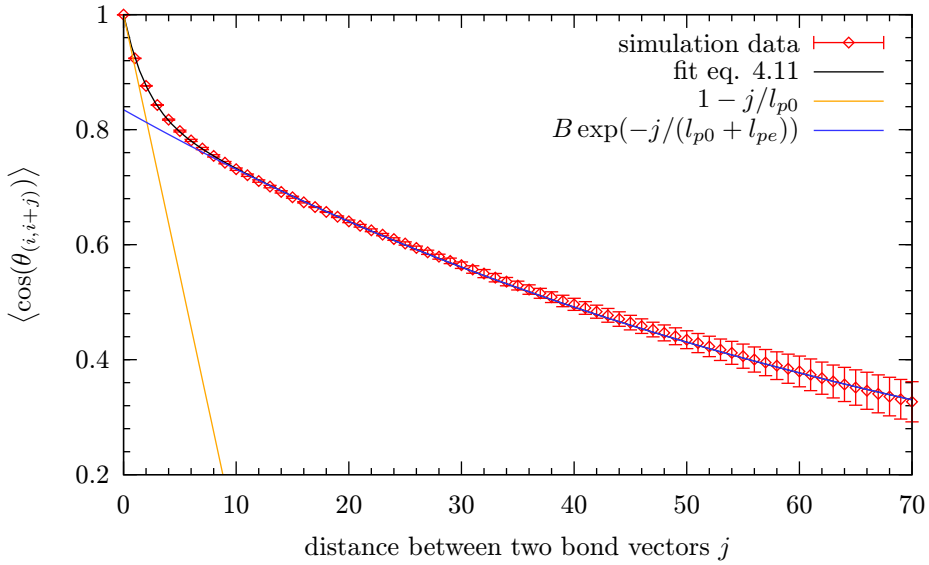

Figure 6.5: The OCF of PE with characteristics: $k_{bend} = 10.0$ and $\kappa = 0.06$. The values of l_p^0 and l_p^e can be found in Tab. 6.1.

Crossover length

The crossover length has a meaning of a distance along the chain, at which the electrostatic repulsion energy of monomeric units and bending energy of the chain become comparable. In Fig. 6.5 we can see the orientational correlation function of a polyelectrolyte with the intrinsic stiffness l_p^0=11.0±0.2 in solution characterized by $\kappa = 0.06$.

For illustration, we plotted two limiting cases of OCF, which express the behaviour of the orientational correlation function at short and long distances. They cross at value of j that corresponds to the crossover length. We obtained the value of s_c directly from the double exponential fit of OCF (see Tab. 6.1).

Barrat and Joanny [39] characterized the local flexibility of the chain by the mean-square value of angle between two bond vectors separated by distance j. The averaged value of the angle $\langle\theta^2(j)\rangle$ is scale-dependent: at distances shorter than crossover length the $\langle\theta^2(j)\rangle$ increases linearly:

$$\langle\theta(j)^2\rangle = \frac{j}{l_p^0}, \tag{6.7}$$

and at longer distances it is described by a function:

$$\langle\theta(j)^2\rangle = \frac{j}{(l_p^0 + l_p^e)} + b. \tag{6.8}$$

From the analysis of bending energy, Barrat and Joanny derived the expression, that describes the $\langle\theta^2(j)\rangle$ as a function of the distance between the bond vectors in the whole range of j [3]. This analysis leads also to the definition of crossover length (eq. 5.9). The validity of the eq. 5.9 was confirmed only for polyelectrolyte systems, that fulfill the condition: $s_c/l_p^0 < 0.2$. For the majority of our simulation data the ratio s_c/l_p^0 is comparable to 0.2. We calculated the crossover length according to eq. 5.9 from the simulation results given in Tab. 6.1 in order to study the applicability of eq. 5.9 for our polyelectrolyte systems. The values of s_c obtained from calculations are in Tab. 6.2.

Another way how to obtain the value of s_c is to fit the simulation data by eq. 6.7 and eq. 6.8. The mean-square value of the angle between two bond vectors is plotted against the distance between them in Fig. 6.6. We can express the crossover length from the parameters that we get from the fit:

$$s_c = \frac{b l_p^0 (l_p^0 + l_p^e)}{l_p^e} \tag{6.9}$$

The acquired values of s_c are summarized in Tab. 6.2. One faces difficulties if he wants to fit the data, because the region of j, where the eq. 6.7 can be applied is very narrow and contains only few points. This method of determination of the crossover length is generally applicable for semiflexible polyelectrolytes, but due to the poor statistics we get only an approximative value of s_c.

For polyelectrolytes, whose intrinsic persistence length is smaller than the electrostatic one, the crossover length should be proportional to the square root of the intrinsic persistence length $s_c \sim \sqrt{(}l_p^0)$. [3] So there is no dependence of s_c on ionic strength of solution (hence on κ) for this group of polyelectrolytes. The condition $l_p^0 < l_p^e$ is satisfied for each of our systems except for systems with high intrinsic stiffness (k_{bend}=32.0, 40.0) and equally high ionic strength ($\kappa > 0.06$), where $l_p^0 \simeq l_p^e$.

In Fig. 6.7, the dependence of s_c on $\sqrt{(}l_p^0)$ is shown. The values of the crossover length obtained from the fit of orientational correlation function lie almost at the same curve. So no matter if the ionic strength of solution is high or low, within the error the polyelectrolyte chains with the same intrinsic stiffness have also the same values of crossover length. This finding is in agreement with previous expectations.

The results obtained from eq. 6.9 are drawn as yellow, green and purple curve. The three curves for different value of κ don't overlap. However, the standard deviations of crossover length are large that we are not able to decide, whether large errors are the reason why the curves don't overlap or it is caused by the fact, that the crossover length depends on κ.

The previous analysis indicates, that the definition of the crossover length derived by Barrat and Joanny (eq. 5.9) is not suitable for polyelectrolyte solutions with $s_c/l_p \simeq 0.2$.

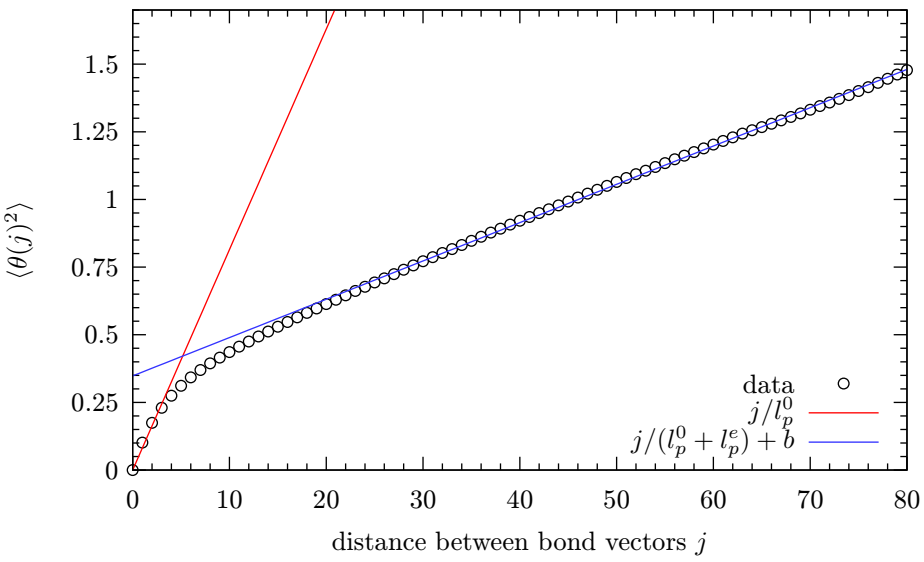

Figure 6.6: The mean-square angle between two bond vectors as a function of a their separation j for PE with characteristics: $k_{bend} = 16.0$ and $\kappa = 0.05$

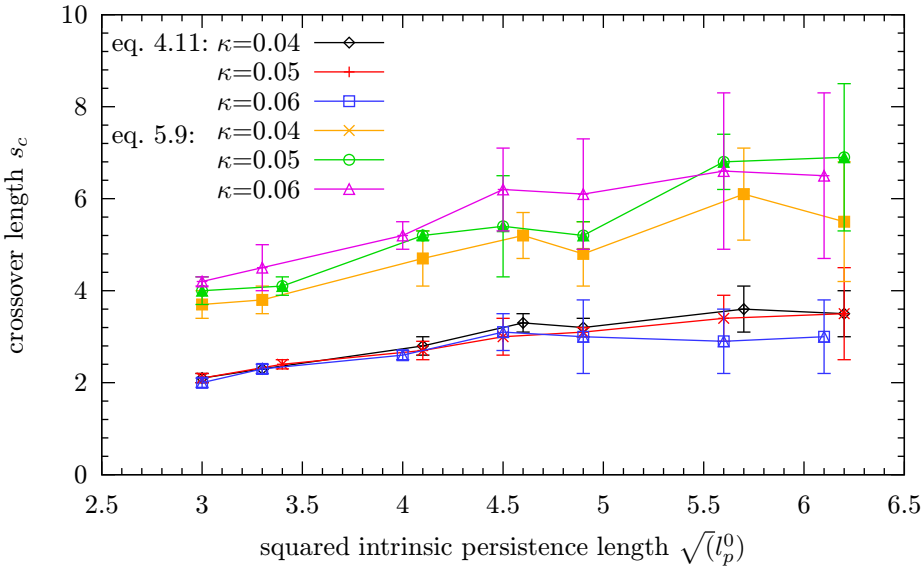

Figure 6.7: The crossover distance as a function of square root of the intrinsic persistence length

The obtained values of s_c are much larger that those from our simulations and moreover they don't show the same tendency as our values of s_c. It is evident from eq. 5.9, that the value of s_c is proportional to the Debye screening length κ^{-1}. This dependence wasn't observed in our simulations. According to Manghi and Netz the value of s_c from the fit of OCF (third column in Tab. 6.2) is equal to that one calculated from eq. 5.9 (fifth column in Tab. 6.2). As we have shown in this section, this assumption is not generally true. For polyelectrolytes, the effective stiffness of which is influenced more by the electrostatic repulsion of monomeric units than by the intrinsic stiffness, the crossover length obtained from the double exponential fit of OCF does not depend on ionic strength of solution.

Table 6.2: The crossover lengths obtained by various methods: from the fit of OCF according to Manghi and Netz (eq. 5.11), from eq 6.9. and from definition 5.9

k_{bend}	κ	s_c from OCF	s_c eq. 6.9	s_c eq. 5.9
8.0	0.04	2.1 ± 0.1	3.7 ± 0.3	6.7
8.0	0.05	2.1 ± 0.1	4.0 ± 0.3	6.1
8.0	0.055	2.0 ± 0.2	4.1 ± 0.3	5.9
8.0	0.06	2.0 ± 0.1	4.2 ± 0.1	5.8
8.0	0.07	2.0 ± 0.1	4.5 ± 0.3	5.5
10.0	0.04	2.3 ± 0.0	3.8 ± 0.3	7.4
10.0	0.05	2.4 ± 0.1	4.1 ± 0.2	6.9
10.0	0.055	2.4 ± 0.2	4.5 ± 0.3	6.5
10.0	0.06	2.3 ± 0.1	4.5 ± 0.5	6.4
10.0	0.065	2.3 ± 0.2	4.9 ± 0.3	6.1
10.0	0.07	2.2 ± 0.4	5.1 ± 0.4	5.9
16.0	0.04	2.8 ± 0.2	4.7 ± 0.6	9.2
16.0	0.05	2.7 ± 0.2	5.2 ± 0.1	8.5
16.0	0.055	2.9 ± 0.1	5.5 ± 0.5	7.9
16.0	0.06	2.6 ± 0.1	5.2 ± 0.3	7.9
16.0	0.065	2.7 ± 0.3	5.7 ± 0.7	7.5
16.0	0.07	2.5 ± 0.3	5.7 ± 0.5	7.5
20.0	0.04	3.3 ± 0.2	5.2 ± 0.5	10.0
20.0	0.05	3.0 ± 0.4	5.4 ± 1.1	9.3
20.0	0.055	3.1 ± 0.1	6.0 ± 0.5	8.8
20.0	0.06	3.1 ± 0.4	6.2 ± 0.9	8.5
20.0	0.065	2.8 ± 0.4	6.1 ± 0.6	8.3
20.0	0.07	3.0 ± 0.8	7.0 ± 0.8	8.0
24.0	0.04	3.2 ± 0.2	4.8 ± 0.7	11.1
24.0	0.05	3.1 ± 0.1	5.2 ± 0.3	10.1
24.0	0.055	2.9 ± 0.2	5.6 ± 0.4	9.5
24.0	0.06	3.0 ± 0.8	6.1 ± 1.2	9.2
24.0	0.065	2.8 ± 0.3	6.7 ± 0.9	8.8
24.0	0.07	2.9 ± 0.7	6.7 ± 1.5	8.5
32.0	0.04	3.6 ± 0.5	6.1 ± 1.0	12.3
32.0	0.05	3.4 ± 0.5	6.8 ± 0.6	10.9
32.0	0.055	3.7 ± 0.8	7.6 ± 1.1	10.5
32.0	0.06	2.9 ± 0.7	6.6 ± 1.7	10.3
32.0	0.065	3.0 ± 0.9	7.1 ± 0.9	9.9
32.0	0.07	2.8 ± 1.5	6.9 ± 2.1	9.5
40.0	0.04	3.5 ± 0.5	5.5 ± 1.3	13.7
40.0	0.05	3.5 ± 1.0	6.9 ± 1.6	12.1
40.0	0.055	3.2 ± 1.1	5.9 ± 2.2	11.4
40.0	0.06	3.0 ± 0.8	6.5 ± 1.8	11.1
40.0	0.065	3.1 ± 2.0	8.1 ± 3.0	10.4
40.0	0.07	3.3 ± 1.5	8.4 ± 1.7	9.9

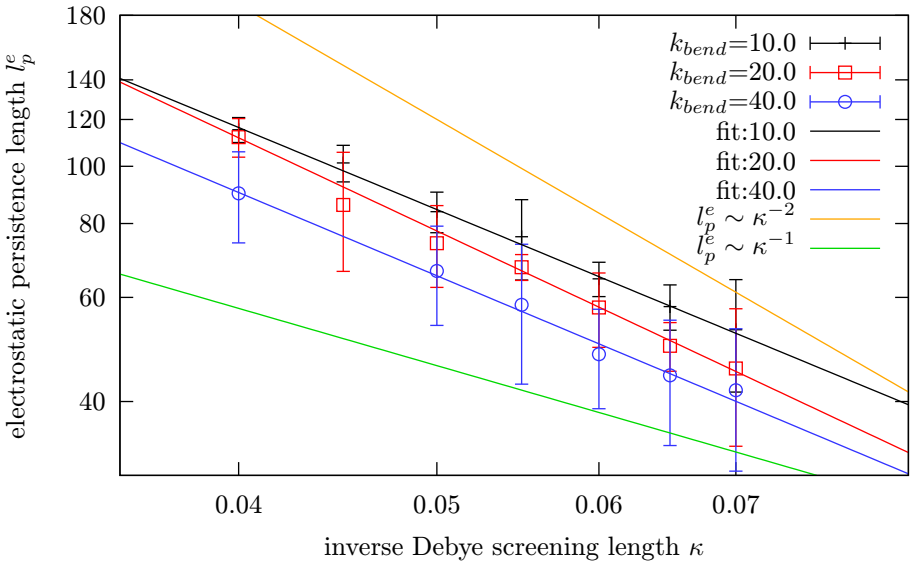

Figure 6.8: Electrostatic persistence length as a function of inverse Debye screening length κ (logarithmic plot)

Electrostatic persistence length

The effect of the salt on the value of the electrostatic persistence length is one of the most discussed problems. The OSF theory predicts the quadratic dependence of the electrostatic persistence length on the Debye screening length (see eq. 5.8). The simulations [14] and theoretical studies [35] proved, that the prediction is valid only for stiff polyelectrolytes. The electrostatic persistence length of flexible polyelectrolytes is thought to be proportional to κ^{-1}.

We studied the dependence of l_p^e on the inverse Debye screening length. The dependencies for three chosen polyelectrolyte systems (three polyelectrolytes with the given intrinsic stiffness in solutions with various ionic strength) are plotted in Fig. 6.8. In the log-log plot the exponent in the relation: $l_p^e \sim \kappa^{-a}$ is equal to slope of the linear function used for the fit:

$$\ln(l_p^e) = a \ln(\kappa) + \text{const.}$$

We determined the value of a for every studied polyelectrolyte system. The obtained average value of the exponent in the dependence of l_p^e on the Debye screening length κ^{-1} is equal to:

$$a = 1.5 \pm 0.1,$$

so we get the relation between the electrostatic persistence length, the Debye screening length and the ionic strength of the solution:

$$l_p^e \sim \kappa^{-3/2} \sim I^{-3/4}. \tag{6.10}$$

Fig. 6.8 includes also the curves for two limiting cases: flexible ($l_p^e \sim \kappa^{-1}$) and stiff polyelectrolytes ($l_p^e \sim \kappa^{-2}$) in order to illustrate the fact, that our simulation data are located between these two limiting cases. It exists no research work aimed at polyelectrolyte solutions with similar characteristics as we have, so it is not possible to compare our results with previous scientific studies. However, for semiflexible polyelectrolytes, one can expect a in the interval: $a \in (1.0, 2.0)$, so the obtained exponent for the dependence

of l_p^e on the Debye screening length is in agreement with the prediction for semiflexible polyelectrolytes.

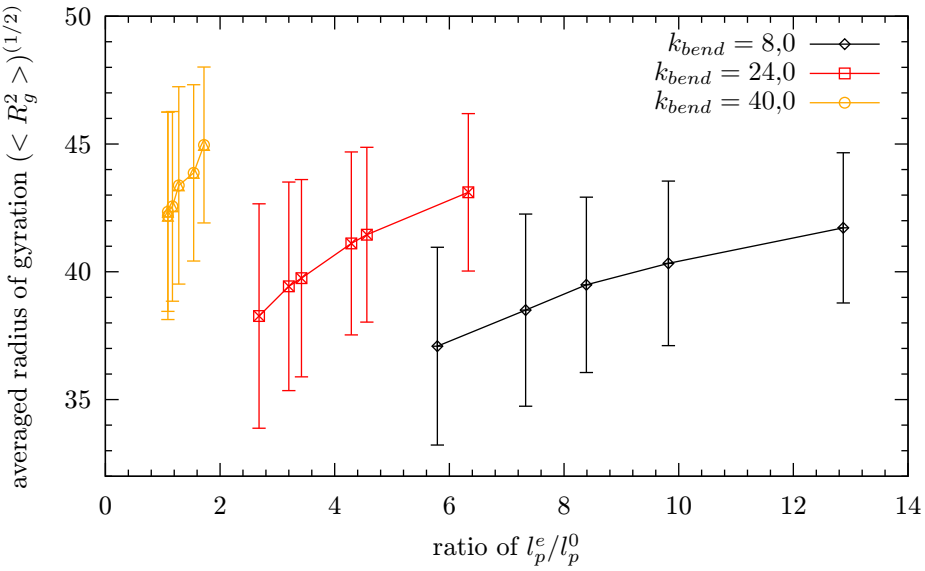

Figure 6.9: Radius of gyration as a function of ratio l_p^e/l_p^0 for chains with bending constants $k_{bend} = 8.0, 24.0, 40.0$

Conformational behaviour of polyelectrolyte chains in solution
We analyzed the variations of the radius of gyration under different conditions in order to get information on the conformational behaviour of the chain in solution. In Fig. 6.9 we see the dependence of the radius of the gyration on the ratio of the electrostatic-to-intrinsic persistence lengths.

Firstly we discuss the change of the chain size with increasing the intrinsic stiffness. As we can see, the polyelectrolyte with the highest intrinsic stiffness ($k_{bend} = 40.0$) has also the highest values of $\sqrt{\langle \mathbf{R}_g^2 \rangle}$. It can be explained by the fact, that an increase in the chain intrinsic stiffness causes the stretching of the chain and forces the chain to form a fully extended configuration.

When the amount of salt added to the solution increases, the ions of salt screen the electrostatic repulsion between the monomeric units and the chain become more flexible, thus its value of $\sqrt{\langle \mathbf{R}_g^2 \rangle}$ decreases. For example, the red curve in Fig. 6.9 shows the decrease of the chain radius of gyration with the decreasing value of electrostatic length (i.e, with the increasing ionic strength).

The size of the chain is affected by the both: the intrinsic and the electrostatic persistence length. Therefore the polyelectrolytes that differ in the intrinsic stiffness and they are in the solutions with different ionic strength can have a very similar radius of gyration. For example, this case occurs for the pair of polyelectrolytes with characteristic $k_{bend} = 24.0$, $\kappa = 0.065$ and $k_{bend} = 8.0$, $\kappa = 0.05$ (see in Fig 6.9 value of $\sqrt{\langle \mathbf{R}_g^2 \rangle} \doteq 40.2$ for both of the chains).

It is important to point out, that although the electrostatic interactions are screened at distances larger than the Debye screening length ($\kappa^{-1} = 14.3 - 25.0$), the electrostatic repulsion between the charged beads influences the chain stiffness far beyond the Debye screening length. At the same time, the stiffness of the chain at large distances depends on

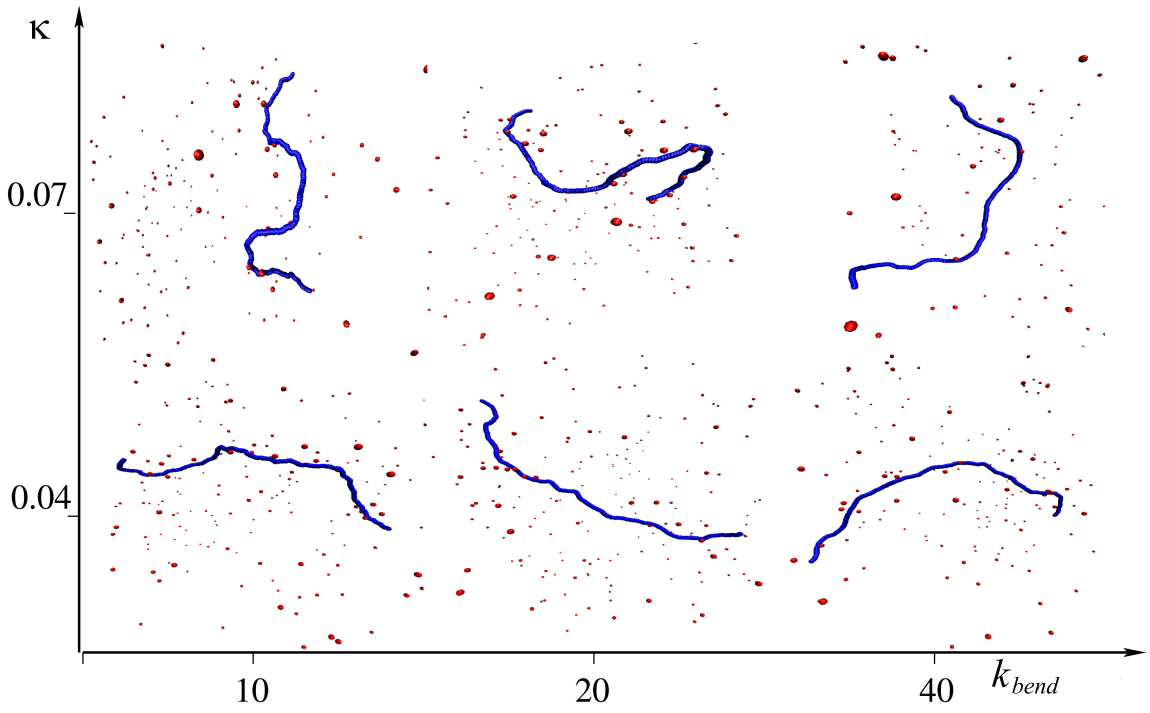

Figure 6.10: Illustration of the change in the chain conformational behaviour under various conditions

intrinsic stiffness of the chain. Therefore we can change the chain conformation by adding the salt only partially. If the value of intrinsic persistence length of the chain is very high, chain behaves like a stiff rod and the increasing of ionic strength of the solution doesn't have a significant effect on the increasing of the chain flexibility, because the contribution of the intrinsic persistence length to the total bending ability of the chain is very high. The demonstration of such a behaviour is in Fig. 6.10. We can observe only slightly conformational changes with increasing of amount of the salt in solution for PE with intrinsic stiffness close to the value 40.0.

So it has to be always taken into account that the stiffness of the chain has a two contributions.

7. Conclusions

In the presented thesis the conformational behaviour of linear semiflexible polyelectrolytes in solutions has been studied. The stiffness of a chain, which is influenced by a number of factors, is characterized by the persistence length. The persistence length has two contributions: the intrinsic l_p^0 and electrostatic l_p^e persistence length.

We obtained the persistence length from the orientational correlation function (OCF) of bond vectors separated by given distance. The double exponential decay of the orientational correlation function predicted theoretically was observed. Results of our simulations were compared with two recently published theoretical approaches. Our results confirm that both approaches describe the OCF at long length scales in agreement with well-known OSF theory, which states that at long distances the total persistence length of the chain corresponds the sum of electrostatic and intrinsic persistence length.

For semiflexible polyelectrolytes a proper description of the orientational correlations at short length scales is essential, what wasn't achieved by the method of Gubarev, Carrillo and Dobrynin. Because the expression for OCF derived by Manghi and Netz allows to explain the properties of OCF at long as well as at short length scales, we used this expression for analysis of OCF calculated from our simulation data.

The intrinsic persistence length obtained from the analysis is proportional to the constant of the bending potential between the chain units, what confirms the results from my bachelor thesis and previous theoretical studies. The crossover distance for the studied polyelectrolyte systems seems to be independent of ionic strength of the solution I. It is in agreement with the prediction for polyelectrolytes, whose electrostatic persistence length is larger than intrinsic one. The obtained electrostatic persistence length scales as $l_p^e \sim I^{-3/4}$, what proves, that the prediction of OSF theory ($l_p^e \sim I^{-2}$) is not valid for semiflexible polyelectrolyte chains.

Our result show that the conformational behaviour of semiflexible polyelectrolytes in solution is controlled by both the electrostatic and intrinsic persistence lengths. The values of the electrostatic persistence length are influenced by the ionic strength of the solution, so the size and conformation of the chain can be modified by adding a salt. For the medium salt regime, that we study, only a small change of the chain conformations can be achieved with the change of ionic strength.

Bibliography

[1] Ducháček V.: *Polymery - výroba, vlastnosti, zpracování, použití*. 2.vydání. Vysoká škola chemicko-technologická v Praze, Praha (2006).

[2] Rubinstein M., Colby R. H.: *Polymer Physics*. Oxford University Press (2003).

[3] Barrat J.L., Joanny J.F.: *Theory of polyelectrolyte solutions*. Advances in Chemical Physics, Vol Xciv 94, p. 1-66 (1996).

[4] Förster S., Schmidt M.: *Physical Properties of Polymers*. Advances in Polymer Science, Vol 120, p. 51-133 (1995).

[5] Smit B., Frenkel D.: *Understanding Molecular Simulations*. Academic, New York (1996).

[6] Grosberg A., Khoklov A.: *Statistical Physics of Macromolecules*. AIP Press, New York (1994).

[7] Ullner M., Woodward C. E.: *Orientational correlation function and persistence lengths of flexible polyelectrolytes*.

[8] Odijk T.: *Polyelectrolytes near the rod limit*. Journal of Polymer Science: Polymer Physics Edition, 15, p. 477-483 (1977).

[9] Skolnick J., Fixman M.: *Electrostatic persistence length of a wormlike polyelectrolyte*. Macromolecules, 10, p. 944-948 (1977).

[10] Goyal S., Perkins N. C., Meiners J. Ch.: *Resolving the Sequence-Dependent Stiffness of DNA Using Cyclization Experiments and a Computational Rod Model*. J. Comput. Nonlinear Dynam., Vol. 3, p. 011003-011009 (2008).

[11] Stellato D.A., Camesano T.A.: *Quantitative analysis of biopolymer conformation using atomic force microscopy: copper-induced conformational changes in poly-g-glutamic acid*.Current Issues on Multidisciplinary Microscopy Research and Education, p. 25-32, Formatex, Badajoz, Spain (2005).

[12] E. Buhler, F. Boué: *Persistence length for a model semirigid polyelectrolyte as seen by small angle neutron scattering: a relevant variation of the lower bound with ionic strength*. The European Physical Journal E - Soft Matter, vol. 10, 2, p. 89-92 (2003).

[13] Reed W.F., Ghosh S., Medjahdi G., Francois J.: *Dependence of polyelectrolyte apparent persistence lengths, viscosity, and diffusion on ionic strength and linear charge density*. Macromolecules, 24, p. 6189-6198 (1991)

[14] Micka U., Kremer K.: *Persistence length of polyelectrolyte chains.* Journal of Physics: Condensed Matter, Vol. 8,, 47, p. 9463-9470 (1996).

[15] Manghi M., Netz R. R.: *Variational theory for a single polyelectrolyte chain revisited.* European Physical Journal E, 14, issue 1, p. 67-77 (2004).

[16] Gubarev A., Carrillo J-M.Y., Dobrynin A.V.: *Scale-Dependent Electrostatic Stiffening in Biopolymers.*Macromolecules, 42, p. 5851-5860 (2009).

[17] Yamakawa H.: *Modern theory of polymer solutions.* Harper and Row, New York (1971).

[18] Müller-Plathe F.: *Coarse-graining in polymer simulation : from the atomistic to the mesoscopic scale and back.* ChemPhysChem,Vol. 3, p. 754-769 (2002).

[19] Doi M., Edwards S. F.: *The theory of polymer dynamics.* The Clarendon Press, Oxford University Press, New York (1986).

[20] Baschnagel J.,Binder K., Doruker P., Gusev A.A., Hahn O., Kremer K., Mattice W.L., Muller-Plathe F., Murat M. Paul W., Santos S., Suter U.W., Tries V.: *Bridging the gap between atomistic and coarse-grained models of polymers: Status and perspectives.* Advances in Polymer Science: Viscoelasticity, Atomistic Models, Statistical Chemistry, 152, p. 41-156, (2000).

[21] Yelash L., Muller M., Wolfgang P., Binder K.: *How Well Can Coarse-Grained Models of Real Polymers Describe Their Structure? The Case of Polybutadiene.*Journal of Chemical Theory and Computation, 2 (3), p. 588 -597, (2006).

[22] Underhill P.T., Doyle P.S.: *On the coarse-graining of polymers into bead-spring chains.*Journal of Non-Newtonian Fluid Mechanics, 122, p. 3-31 (2004).

[23] Limbach H., Arnold A., Mann B. A., Holm C.: *ESPResSo - An Extensible Simulation Package for Research on Soft Matter Systems.* Computer Physics Communications, 174, p. 704-727 (2006).

[24] Nezbeda I., Kolafa J., Kotrla M.: *Úvod do počítačových simulací. Metody Monte Carlo a molekulární dynamiky.* Karolinum, Praha (1998).

[25] Allen M. P.: *Introduction to Molecular Dynamics Simulation.* Computational Soft Matter: From Synthetic Polymers to Proteins, Lecture Notes, John von Neumann Institute for Computing, Julich, NIC Series, Vol. 23, p. 1-28 (2004).

[26] Bennemann C., Paul W., Binder K., Dünweg B.: *Molecular Dynamics Simulations of the Thermal Glass Transition in Polymer Melts: Alpha-Relaxation Behaviour.*Physical Review E, Vol. 57, p. 843–851 (1998).

[27] Dobrynin A. V.: *Electrostatic Persistence Length of Semiflexible and Flexible Polyelectrolytes.* Macromolecules, 38, p. 9304-9314 (2005).

[28] Stevens M.J., Kremer K.: *Structure of Salt-free Linear Polyelectrolytes in the Debye-Hückel Approximation.*Journal de Physique II, Vol. 6, Issue 11, p. 1607-1613 (1996).

[29] Reddy G., Yethiraj A.: *Implicit and Explicit Solvent Models for the Simulation of Dilute Polymer Solutions.* Macromolecules, 39, p. 8536-8542 (2006).

[30] Hűnenberger P. H.: *Thermostat Algorithms for Molecular Dynamics Simulations.* Advanced Computer Simulation, Vol. 173, p. 105-149 (2005).

[31] Manning G.S.: *Counterion condensation on a helical charge lattice.* Macromolecules, 34, p.4650-4655 (2001).

[32] Dobrynin A.V., Rubinstein M.: *Theory of polyelectrolytes in solutions and at surfaces.* Progress in Polymer Science, 30, p. 1049-1118 (2005).

[33] *IUPAC Compendium of Chemical Terminology - the Gold Book*, 2nd edition (1997). `www.iupac.org/goldbook/P04515.pdf`

[34] Hsu H.-P., Paul W., Binder K.: *Standard Definitions of Persistence Length Do Not Describe the Local Intrinsic Stiffness of Real Polymer Chains.*Macromolecules, Vol. 43, p. 3094-3102 (2010).

[35] Ullner M., Jönsson B., Peterson C., Sommelius O., Söderberg B.: *The Electrostatic Persistence Length Calculated from Monte Carlo, Variational and Perturbation Methods.*Journal of Chemical Physics, Vol. 107, p. 1279-1287 (1997).

[36] Bačová P.: *Study of persistence length of linear polyelectrolytes in solutions.* Bachelor thesis (2008).

[37] Micka U., Kremer K.: *Persistence length of weakly charged polyelectrolytes with variable intrinsic stiffness.* Europhysics Letters, 38, p. 279-284 (1997).

[38] Everaers R., Milchev A., Yamakov V.: *The Electrostatic Persistence Length of Polymers beyond the OSF Limit.* The European physical journal E - Soft matter, p. 3-14 (2002).

[39] Barratt, J. L., Joanny, J. F.: *Persistence Length of Polyelectrolyte Chains* Europhysics Letters, 24, p. 333-338 (1993).

[40] Ullner M.: *Comments on the scaling behavior of flexible polyelectrolytes within the Debye-Huckel approximation.*Journal of Physical Chemistry B, Vol. 107, p. 8097-8110 (2003).

[41] M. Schmidt: *Polyelectrolytes with defined molecular architecture I*, Advances in polymer science vol. 165, Springer, New York, NY (2004).

[42] Podesta A., Indrieri M., Brogioli D., Manning G. S., Milani P., Guerra R., Finzi L., Dunlap D.: *Positively Charged Surfaces Increase the Flexibility of DNA* Biophysical Journal, vol.89, p. 2558-2563 (2005).

[43] Zhongde X., Hadjichristidis N., Fetters L.J., Mays J.W.: *Structure/chain-flexibility relationships of polymers.* Advances in Polymer Science, Vol. 120, p. 1-50 (1995).

[44] Schäfer L., Elsner K.: *Calculation of the persistence length of a flexible polymer chain with short-range self-repulsion.* The European physical journal. E, Soft matter, 13, p. 225-237 (2004).

[45] Cannavacciuolo L., Pedersen J. S.: *Properties of polyelectrolyte chains from analysis of angular correlation functions.* The Journal of chemical physics, Vol. 117, p. 8973-8982 (2002).